TITLE PAGE

Title: Water levels affect photosynthesis and nutrient use more than salinity in a scrub Red Mangrove forest of the southeastern Florida Everglades

Authors: J. Aaron Hogan[1*], Edward Castañeda-Moya[2], Lukas Lamb-Wotton[1], Christopher Baraloto[1]

Author Affiliations: [1] Department of Biological Sciences, Florida International University, Miami, FL USA 33199; [2] Institute of Environment, Florida International University, Miami, FL USA 33199

* *Corresponding Author:* J. Aaron Hogan, email: jhogan@fiu.edu

ORCiDs:

J. Aaron Hogan: 0000-0001-9806-3074; Edward Castañeda-Moya: 0000-0001-7759-4351; Lukas Lamb-Wotton: 0000-0002-0712-9005, Baraloto: 0000-0001-7322-8581

Authorship statement: The conception and design of the study and the acquisition of data were conducted by JAH, EC-M, and LL-W. Data analyses were performed by JAH and EC-M. Interpretation of the data was carried out by JAH, EC-M, LL-W, TT, and CB. The manuscript was drafted by JAH with the help of EC-M. All authors have contributed to the final version of the manuscript and have approved its submission to the journal.

Data deposition: The data collected and used in this study have been archived and are available through the Environmental Data Initiative data repository:
Hogan, J.A., E. Castaneda, and L. Lamb-Wotton. 2021. FCE LTER Taylor Slough/Panhandle-7 Site Scrub Red Mangrove (Rhizophora mangle) Leaf Gas Exchange Data, Florida, USA from January-December 2019 ver 1. Environmental Data Initiative.
https://doi.org/10.6073/pasta/27f6332609eb1ef6d398c7855855f2e3 (Accessed 2021-01-26).
Note: this data archive also contains R code for running the linear mixed effects models using the archived datasets.

ABSTRACT

Photosynthesis is an essential process to mangrove forest carbon cycling, which plays a critical role in the global carbon cycle. We investigated how differences in mangrove island micro-elevation (i.e., habitat) affect tree physiology in a scrub mangrove forests of the southeastern Everglades. We measured leaf gas exchange rates of scrub *Rhizophora mangle* trees monthly during 2019, hypothesizing that CO_2 assimilation (A_{net}) and stomatal conductance (g_{sw}) would decline with increases in water level and salinity, with larger differences at mangrove islands edges than centers, where inundation and salt stress are greatest. Water levels varied between 0 and 60 cm, rising during the wet season (May-October) relative to the dry season (November-April). Porewater salinity ranged from 15 to 30 ppt, being higher at mangrove island edges compared to centers. A_{net} maximized at 15.1 µmol m^{-2} $s^{-1,}$ and g_{sw} was typically <0.2 mol m^{-2} s^{-1}, both of which were greater in the dry than the wet season and greater at mangrove island centers than edges. After accounting for season and habitat, water level had a positive effect on A_{net} in both seasons, but no effect on g_{sw}. Similarly, porewater salinity had a slightly positive marginal effect on A_{net} but a negligible effect on g_{sw} Our findings suggest that water levels drive variation in A_{net} more than salinity in Everglades scrub mangroves, while also constraining A_{net} more than g_{sw}, and that the interaction between permanent flooding and habitat varies with season as physiological stress is alleviated at higher-elevation mangrove island center habitats in the dry season. Additionally, habitat heterogeneity leads to differences in nutrient and water acquisition and use between trees growing in island centers versus edges, creating distinct physiological controls on leaf physiology and photosynthesis which could ultimately affect carbon flux dynamics of scrub mangrove forests across the Everglades landscape.

Keywords: Scrub mangroves, Florida Coastal Everglades, photosynthesis, porewater salinity, hydroperiod, *Rhizophora mangle*.

INTRODUCTION

Global climate change is affecting costal ecosystems in an unprecedented manner, principally through flooding and saltwater intrusion (Pezeshki et al 1990a, Yu et al 2020). Increases in flooding severity and salinity due to sea-level rise have the potential to push ecosystems to degraded alternative stable states, where biogeochemical cycles and ecosystem function including carbon sequestration and storage potential are impaired (Neubauer et al., 2013, Tully et al. 2019, Yu et al 2020). Mangrove wetlands are particularly susceptible to sea-level rise because of their position at the boundary between terrestrial and marine ecosystems (Field 1995, Ellison and Farnsworth 1997). Although they cover <1% of the Earth's surface (Giri et al. 2011), mangroves forests are among the most productive ecosystems in the world, playing disproportionately large role in the global carbon cycle (Twilley et al. 1992, Jennerjahn and Ittekkot 2002, Bouillon et al. 2008, Donato et al. 2011). Furthermore, mangroves mitigate atmospheric greenhouse gas accumulation through carbon sequestration and storage in vegetation and soil (Mcleod et al. 2011, Murdiyarso et al. 2015, Lovelock et al. 2017, Rovai et al. 2018). Global patterns in mangrove forest structure and function are controlled by regional climate and geophysical processes (e.g., river input, tidal amplitude, wave energy –Thom 1982, Woodroffe 1992, Twilley 1995, Rovai et al. 2016, Ribeiro et al. 2019, Simard et al. 2019), which potentially modulate the effects of global change drivers (i.e., sea-level rise and saltwater intrusion) on mangrove tree physiology. Mangrove species have developed large variation in key life-history traits, such rates of photosynthesis, water-use and nutrient-use efficiencies, and growth rates and biomass allocation ratios in response to the interactions among resource (e.g., light and nutrients), regulators (e.g., salinity, sulfides), and hydroperiod gradients (e.g., frequency, depth and duration of inundation – Twilley and Rivera-Monroy 2005, Alongi 2008, Twilley and Rivera-Monroy 2009, Castañeda-Moya et al. 2013).

Scrub mangrove forests, dominated by *Rhizophora mangle,* are common in Caribbean karst environments (e.g., Florida, Puerto Rico – Cintron et al. 1978, Lugo and Snedaker 1974). The stunted physiognomy (i.e., reduced growth and development) of scrub mangroves results from severe nutrient (e.g., phosphorus, P) limitation, prolonged or permanent inundation with little tidal influence, and seasonal water stress (Feller 1995, Koch and Snedaker 1997, Cheeseman and Lovelock 2004, Medina et al. 2010, Castañeda-Moya et al. 2013). Scrub mangrove forests develop distinct landscape patterning, forming mangrove island clusters with higher elevations than their surrounding shallow open-water ponds and channels (Figure 1A). Elevational differences are maintained through the vertical accumulation of biogenic material via

root biomass and production, leaf litter accretion and wood deposition (McKee et al. 2007, McKee 2011, Krauss et al. 2014). For example, in scrub mangrove islands of the southeastern Everglades, island center habitats have 66% more root biomass and 52% more root production than island edges (Castañeda-Moya et al. 2011), which leads to spatial differences in soil elevation among island habitats. These differences in soil elevation interact with environmental gradients (e.g., salinity, hydroperiod) along the intertidal zone in complex ways to affect mangrove physiology (i.e., rates of net CO_2 assimilation – A_{net}, growth rates, or sap flux) at variable scales, from the leaf to the ecosystem and landscape levels (Medina and Francisco 1997, Twilley et al. 1998, Medina et al. 2010, Twilley et al. 2017). This is particularly significant to the South Florida region given that most of the mangrove cover and standing biomass in the coastal Everglades is associated with scrub forests (Simard et al. 2006, Rivera-Monroy et al. 2019), which are distributed across a broad range of environmental conditions.

Because mangrove forests are usually inundated, hydrology (e.g., water levels and flooding duration) is a critical driver controlling mangrove wetlands structural and functional attributes, and therefore, carbon dynamics, and other biogeochemical processes across spatial and temporal scales (Medina 1999, Castañeda-Moya et al. 2013, Twilley et al. 2017, 2019, Zhao et al. 2020). Although mangrove species are tolerant to flooded conditions, they are still susceptible to flooding damage if plants become completely submerged for days to weeks (Wanless 1998, Mendelssohn and McKee 2000, McKee 2011). Inundation stress typically decreases plant carbon uptake and storage, due to interactions between inundation duration and mangrove transpiration rates; hence A_{net} and growth rates are usually depressed in mangrove forests subjected to longer flooding duration (He et al. 2007, Cardona-Olarte et al. 2013). For example, greenhouse studies have revealed a 20% reduction in maximum A_{net} when mangrove seedlings and saplings were subjected to short-term intermittent seawater flooding (6 to 22 days, Krauss et al. 2006). Mangrove physiology is further affected by how seawater flooding interacts with fresh water and nutrient inputs (Wolanski 1992). For instance, studies have shown a reduction in stomatal conductance (g_{sw}) and leaf water potential in *Bruguiera gymnorrhiza* seedlings when exposed to prolonged flooding for up to 80 days with 33% seawater compared to the control plants; however, seedlings flooded with fresh water for 80 days showed an increase in both parameters (Naidoo 1983). In contrast, seedlings of *Avicennia germinans* and *Laguncularia racemosa* exposed to permanent flooding with 23% seawater showed a reduction in leaf area, with no effect on g_{sw}, A_{net}, or water use efficiency (Krauss et al. 2006). Hydrologic conditions can further negatively influence mangrove physiology through the interaction with soil phytotoxins (i.e., sulfides), produced as by-products of low oxygen

availability and the soil redox conditions related to permanent flooding, which can potentially depress water and nutrient uptake (Nickerson and Thibodeau 1985, McKee 1993, Ball 1996, Pezeshki and DeLaune 2012, Lamers et al. 2013).

Mangroves are highly adapted to tolerate salt stress, with salinity exerting the greatest impact on forest productivity, tree growth rates, and species composition and zonation with effects particularly evident along steep salinity gradients in the intertidal zone (i.e., those >30 ppt), and in dry environments (Lugo and Snedaker 1974, Cintron et al. 1978, Medina and Francisco 1997, Castañeda-Moya et al. 2006, Reef and Lovelock 2015). Salt stress variably affects mangrove tree physiology, depending on species-specific salt tolerance levels and mechanisms to process salt (Parida and Jha 2010, Reef and Lovelock 2015). For example, *R. mangle* may naturally inhabit environments in the neotropics with salinities from near zero (e.g., riverine mangroves) to around 35 ppt (e.g., fringe mangrove forests). Still, *R. mangle* can also be found in dry coast environments (e.g., southern Puerto Rico, Pacific coast of Honduras) with salinities up to 50-60 ppt (Cintron et al. 1978, Cardona-Olarte et al. 2006). *R. mangle* is a non-excreting salt extruder because its roots largely prevent salt from entering the plant. It lacks the excretory glands that other mangrove species (e.g., *L. racemosa*) use to excrete salt. As such, the xylem of *R. mangle* is 100 times less saline than seawater (Scholander et al. 1962, Scholander 1968, Medina and Francisco 1997, Tomlinson 2016) because of ultrafiltration by cell membranes in the thick aerenchyma and cortical layers of its root tissues (Field 1984, Werner and Stelzer 1990). However, some salt still enters the plant through the roots, which has a deleterious effect on the physiology of *Rhizophora* trees, causing decreases in growth and A_{net} rates, and water and nutrient use efficiencies (Ball 1988, Clough and Sim 1989, Lugo et al. 2007, Medina et al. 2010, Cardona-Olarte et al. 2013).

Mangrove A_{net} varies widely with environment (e.g., water and salinity levels), mangrove stature (e.g., fringe vs. basin ecotypes – *sensu* Lugo and Snedaker 1974), and nutrient availability. A_{net} for *R. mangle* maximizes around 20 µmol m^{-2} s^{-1} (Golley et al. 1962, Bjorkman et al. 1988, Lin and Sternberg 1992, Lovelock and Feller 2003, Lugo et al. 2007, Ball 2009); however, A_{net} for scrub mangroves is lower, generally ranging from <5 µmol m^{-2} s^{-1} (Golley et al. 1962, Cheeseman et al. 1997, Cheeseman and Lovelock 2004) to roughly 13 µmol m^{-2} s^{-1} (Lugo et al. 2007, Barr et al. 2009). A field study from Jobos Bay in southern Puerto Rico demonstrated a significant decrease in *R. mangle* A_{net} (from 12.7 to 7.9 µmol m^{-2} s^{-1}) and g_{sw} (from 0.28 to 0.19 µmol m^{-2} s^{-1}) when comparing fringe habitats at 35 ppt salinity to inland salt flat habitats at 80 ppt (Lugo et al. 2007). Reductions in A_{net} and g_{sw} were accompanied by

changes in leaf morphology (i.e., smaller specific leaf area, SLA), reduced nutrient-use efficiency, and increased nutrient resorption, which demonstrates how environmental effects on mangrove physiology can have consequences for ecosystem biogeochemical cycles. Thus, increasing salinity decreases A_{net} and g_{sw} and increases photosynthetic water use efficiency (*wue*) in mangroves, with *Rhizophora* species exemplifying these trends (Ball 2009, Clough and Sim 1989). Moreover, the high salt tolerance capacity of mangroves leads to interesting dynamics between A_{net} and water use (Sobrado 2000, Lovelock and Feller 2003, Ball 2009). For instance, *R. mangle* has very succulent leaves with lower *wue* compared to more salt-tolerant species (i.e., *A. germinans* or *L. racemosa*); however, *R. mangle* has greater efficiency of water transport in stems than more salt-tolerant species (Sobrado 2000). Thus, when considering the effects of salinity on leaf gas exchange rates, plant water use must be considered in concert because both A_{net} and g_{sw} decline in a similar fashion with increasing salinity, effectively creating co-limitation of photosynthesis at moderate to high salinities (Ball 2009).

In mangrove forests of the Florida Everglades, variation in environmental gradients including hydroperiod (e.g., duration of inundation) and soil P fertility controls mangrove vegetation patterns and ecological processes (e.g., litterfall production) across the coastal landscape (Chen and Twilley 1999; Castañeda-Moya et al. 2011, 2013). However, it is not completely understood how the interaction between water level dynamics and salinity affect *in situ* rates of leaf gas exchange of mangrove in this region. Experimental evidence using *R. mangle* seedlings from south Florida showed that inundation created a greater degree of physiological stress than did salinity levels; however, salinity accelerated the adverse effects of inundation stress on leaf function over time (Cardona-Olarte et al. 2013). In contrast, other studies have reported no clear effect of water levels or flooding duration on rates of mangrove gas exchange, although inundation duration decreased variability in leaf gas exchange measurements (Hoppe-Speer et al. 2011). Using Florida mangroves, Krauss et al. (2006) found that short-term intermittent flooding decreased rates of leaf gas exchange relative to unflooded or permanently flooded greenhouse-grown seedlings, but that for *in situ* established *R. mangle* saplings growing along a natural tidal inundation gradient in Shark River estuary in the southwestern Everglades, flooding led to increases in A_{net} and *wue*. Permanent flooding leads to decreases in A_{net} and g_{sw} rates in most wetland plants (Kozlowski 1997); however, how inundation dynamics interact with salinity along the intertidal zone to influence mangrove physiology at different spatial and temporal scales in south Florida mangroves remains largely unknown. Further, global change driven sea-level rise and saltwater intrusion in South Florida

coupled to large-scale freshwater diversion has accelerated mangrove encroachment into inland freshwater wetlands over the past 60 years (Ross et al. 2000). As sea levels will continue to rise, it is imperative to further our understanding of the effects of inundation and salinity on mangrove physiology and subsequent ecosystem functioning (e.g. carbon flux) in the region.

Here, we present a comprehensive, one-year analysis of the spatial and seasonal effects of salinity (surface and porewater) and water levels on photosynthetic responses of *R. mangle* scrub mangroves in southeastern Florida Everglades. We focused our sampling on mangrove islands with noticeable micro-elevational differences between the center and edge to understand the influence of water levels and salinity on *R. mangle* tree physiology. We addressed the following questions: (1) how do rates of leaf gas exchange (e.g., A_{net}, g_{sw}) vary with mangrove island micro-elevation (center vs. edge habitats)? (2) how does leaf gas exchange respond to seasonal changes in surface and porewater salinity and water level? (3) how do water- and nutrient-use efficiencies of *R. mangle* leaves vary between mangrove island center and edge habitats. We hypothesized that A_{net} would be greater for *R. mangle* leaves located in higher elevation center habitats relative to lower elevation mangrove edges. We also expected that A_{net} should vary little with season (i.e., <2 µmol CO_2 m^{-2} s^{-1}) and that seasonal variation in g_{sw} would be less than variation in A_{net}, relative to the range of variability among leaves because of strong control on g_{sw} by *R. mangle.* Moreover, given that scrub mangroves in Taylor River basin are strongly limited by phosphorus (i.e., soil N:P = 102-109 – Castañeda-Moya et al. 2013), they should have high rates of P resorption. Finally, we predicted that mangrove island centers function at a higher physiological level (i.e., with greater rates A_{net} and g_{sw}) due to lower levels of inundation and salt stress. Thus, mangrove trees in island centers should have greater *wue* (Ball 2009) and higher relative rates of nutrient resorption (Lugo et al. 2007, Medina et al. 2010) than trees at island edges.

METHODS

Study Site

This study was conducted in the southeastern region of Everglades National Park in a mangrove site known as Taylor Slough/Panhandle-7 (TS/Ph-7: 25.197°N, 80.642°W, Figure 1B), one of the six mangrove sites established in 2000 as part of the Florida Coastal Everglades Long-Term Ecological Research (FCE-LTER) program (Childers 2006; http://fcelter.fiu.edu). TS/Ph-7 is located approximately 1.5 km inland from Florida Bay in the downstream portion of the Taylor River. Mangroves zones at TS/Ph-7 are dominated by scrub *Rhizophora mangle* L.

trees, with clusters of *Laguncularia racemosa* L. and *Avicennia germinans* (L.) L. intermixed with low densities of freshwater grasses *Cladium jamaicense* (Crantz) Kük and *Eleocharis cellulosa* Torr. (Loveless 1959). Mangrove tree heights reach 1.5 to 2 m (Ewe et al. 2006).

The substrate at this site is organic mangrove peat soil (~1 m depth) overlying the karstic bedrock (depth ~1.5-2 m, Table 1; Castañeda-Moya et al. 2011, Ewe et al. 2006). Surface (0-45 cm depth) soils at TS/Ph-7 have high organic matter content (71%), low bulk density (0.16 g cm^{-3}), low total nitrogen (TN, 2.5 mg cm^{-3}) and low total phosphorus (TP, 0.06 mg cm^{-3}) concentrations, resulting in a highly P-limited environment with soil N:P ratios of about 102 (Castañeda-Moya et al. 2013). Mangrove zones in Taylor River are permanently flooded for most of the year, with an average annual flooding duration averaging 360 d yr^{-1} from 2001 to 2005. This results in anoxic soil conditions and a buildup of porewater sulfide (range: 0.5-2 mM) throughout the year that constrains mangrove growth (Castañeda-Moya et al. 2011, 2013). The tidal effect is negligible in Taylor River, and water flow and hydrology are determined by seasonal precipitation, upland runoff, and wind (Michot et al. 2011, Sutula et al. 2001). The interaction between low P fertility and permanent flooding conditions results in the formation of scrub forests with restricted tree height and aboveground productivity, and high root biomass allocation and high root: shoot ratios compared to riverine mangrove forests along Shark River estuary in southwestern FCE (Ewe et al. 2006, Castañeda-Moya et al. 2011, 2013, 2020).

South Florida has a subtropical savanna climate per the Köppen climate classification, where the average air temperature is between 20 and 30°C and relative humidity is high (70-80%). Rainfall and evapotranspiration vary interannually and average 1500 and 1300 mm $year^{-1}$, respectively (Abiy et al. 2019). In the Everglades, 60% of the precipitation occurs during the wet season, and only 25% during the dry season (Duever et al. 1994). Analysis of long-term (110-year) rainfall trends for South Florida has shown that the annual hydrologic regime can be divided into two seasons: a wet season from May to October and a dry season from November to April (Abiy et al. 2019). For the 2019 calendar year, temperature and relative humidity data were collected from an eddy covariance flux tower installed at TS/Ph-7 and operational since December 2016. Rainfall data were collected from a nearby meteorological station (station name: “Taylor_River_at_mouth”) managed by the US Geological Survey as a part of the Everglades Depth Estimation Network (https://sofia.usgs.gov/eden).

Experimental Design

Due to the stunted physiognomy of the forest at TS/Ph-7, eight distinct mangrove islands of similar size (3-5 m in diameter) were selected and treated as experimental units for repeated measurements of leaf photosynthesis and physicochemical variables from January to December 2019. Mangrove islands were selected within previously-established permanent vegetation plots (two 20×20m plots) based on their location relative to the shoreline (i.e., Taylor River), with four islands located in the fringe mangrove zone (~50-60 m from the edge) and four islands located in the interior forest (~100-110 m inland; Figure 1B). Mangrove islands with distant micro-elevational gradients were selected, having higher soil elevation center habitats and lower elevation edge habitats. Mangrove islands are surrounded by open water ponds (Figure 1A) and remain flooded for most of the year, except the center island habitats during the dry season (Castañeda-Moya et al. 2011, 2013, Figure S1).

Within each mangrove island, a higher-elevation center and a lower-elevation edge habitat were each permanently marked with an aluminum rod exposed 1.5 m above the soil surface and buried approximately 1 m below the soil surface. Soil surface elevation was measured for all mangrove islands at both habitats, in addition to six measurements in the adjacent shallow ponds surrounding mangrove islands. Measurements were taken using real-time kinematics referenced to the 1988 North American Vertical Datum (NAVD88) with a Trimble R8 global navigation satellite system receiver (Trimble; Sunnyvale, CA, USA), which has a horizontal accuracy of ±1 cm and vertical accuracy of ±2 cm.

Water level and salinity measurements

Water levels relative to the soil surface were measured monthly with a meter stick at each of the permanent aluminum rods established at all island habitats. A porewater sample was collected at 30 cm depth at each habitat using a 60 ml syringe attached to a stopcock and a rigid tubing probe (3/16" Ø; McKee et al. 1988). Porewater temperature and salinity were measured using a handheld YSI conductivity-salinity-temperature meter (model Pro 30, YSI Inc., Yellow Springs, OH, USA). A sample of surface water (when present) was also collected at each island habitat to measure salinity and temperature. Continuous measurements of water levels and salinity have been recorded at this site since December 2000, which were used to confirm trends in water level measurements made by hand (see Figure S2 for details).

Photosynthesis measurements

Photosynthetic gas exchange measurements of *R. mangle* leaves were conducted once a month (9:00 AM to 1:00 PM) at eight scrub mangrove islands from January to December 2019

using a Li-COR Li-6800 portable photosynthesis system (Li-COR Inc., Lincoln, NE, USA). At each island habitat (center vs. edge), five mature green leaves were randomly selected from top mangrove branches. Fully developed and healthy (i.e., without herbivory) green leaves from the second-most distal pair of leaves on the leaf rosette were chosen. The Li-6800 was clamped onto each leaf and held until machine stability was reached, wherein data points were logged.

The environmental configuration of the Li-6800 was: flow rate of 600 µmol s^{-1}, 50-70% relative humidity of the incoming air (slightly drier than ambient air to prevent condensation in the instrument), 400 µmol mol^{-1} CO_2 concentration, and light level of 1000 µmol m^{-2} s^{-1}, which was determined to be non-limiting and similar to ambient environmental conditions. We used five stability criteria, which were all assessed over a 15 s interval: the slope of A_{net} being <1 µmol m^{-2} s^{-1}, the slope of the concentration of intracellular CO_2 (c_i, which is a calculated parameter using the difference in CO_2 concentrations between IRGAs in the Li-6800) being < 5 µmol mol^{-1}, the slope of g_{sw} being < 0.5 mol m^{-2} s^{-1}, the slope of the transpiration rate (E) being less than 1 mol m^{-2} s^{-1}, and the slope of the difference in air water vapor concentration between the sample and reference IRGA (ΔH_2O) being less than 1 mmol mol^{-1}. Air (or leaf) temperature within the leaf chamber was not controlled, but allowed to vary with the ambient conditions at the site, ranging from 26.1 to 32.0°C. We calculated *wue* as the ratio of leaf CO_2 uptake to water loss (i.e. $A_{net}/g_{sw}/1000$).

Measurement of leaf functional traits, nutrient content, and isotopic signatures

During the monthly photosynthesis measurements in February, May, August, and November, measured mature green leaves (n = 5 per habitat, 40 in total) were collected at half of the island (four of the eight islands with two per location) for determination of leaf functional traits and total carbon (TC), nitrogen (TN), and phosphorus (TP) content. Leaves were numbered, placed in a sealed, moist bag to prevent water loss, and transported to the laboratory in a cooler with ice for further analyses. Five senescent leaves were also collected from the same islands at the same time to determine carbon and nutrient content. At the laboratory, leaves were removed from bags, dried, and immediately weighed to obtain leaf fresh mass. Leaves were then scanned at high resolution and oven-dried for at least 72 hours at 60°C to constant weight before recording their dry mass. Leaf area was measured using ImageJ (Schneider et al. 2012). Leaf dry mass was recorded and used to calculate leaf dry matter content (LDMC) as the ratio of the dry leaf mass (in mg) to its fresh mass (in g, mg g^{-1}), percent leaf water content (1000-LDMC; %), and SLA, the ratio of leaf dry weight to leaf area (cm^2 g^{-1}). These methods followed Corneilissen et al (2003).

For nutrient analyses, composite leaf samples containing the five leaves from each island habitat per collection were ground into a fine powder using a vibrating ball mill (Pulversette 0, Frtisch GmbH, Idar-Oberstein, Germany). Green and senescent leaf samples were stored in scintillation vials at room temperature and analyzed separately. Leaf TC and TN content were determined for each sample with a NA1500 elemental analyzer (Fisons Instruments Inc., Danvers, MA, USA). TP was extracted using an acid-digest (HCl) extraction, and concentrations of soluble reactive P were determined by colorimetric analysis (Methods 365.4 and 365.2, US EPA 1983). Leaf C and N bulk isotopic signatures ($\delta^{13}C$, $\delta^{15}N$) were analyzed on a Thermo Scientific Delta V Plus CF-IRMS coupled to an 1108 elemental analyzer via a ConFlo IV interface (Thermo Fisher Scientific, Waltham, MA, USA). All C and N analyses were conducted at the Southeast Environmental Research Center Analysis Laboratory (SERC-NAL). SERC-NAL follows strict internal and external QA assurance practices and is NELAC Certified for non-potable-water-General Chemistry under State Lab ID E76930.

Using leaf carbon isotope fractionation values, we calculated the concentration of intracellular CO_2 and plant water use efficiency integrated over the lifespan over the leaf (i.e., intrinsic water use efficiency, *WUE*) via methods described by O'Leary (1988) and Marshall et al. (2007) (and outlined in Lambers et al. 2008). We used an ambient concentration of atmospheric CO_2 of 408 µmol mol^{-1} for our calculations, which is a conservative estimate for the 2019 calendar year and was indicative of the atmospheric conditions at the site. Thus, the equation used to calculate c_i and *WUE* from carbon isotope data were: $c_i = ((-8.5 - \delta^{13}C - 4.4) \div 22.6) \times 408)$, and $WUE = (408 \times (1 - c_i \div 408)) \div 1.6$, where c_i is the value derived from the previous equation. Additionally, the following equation was used to calculate resorption of N and P using green (G) and senescent (S) leaf nutrient content: Relative resorption (%) = ((G - S) ÷ G × 100) (Pugnaire and Chapin 1993).

Statistical Analyses

Repeated measures Analysis of Variance (ANOVA) was used to test for differences in water level, surface water salinity, and porewater salinity among locations (fringe and interior), island habitats (center and edge), and season (wet and dry), as well as for the interaction between these effects and season, which was used as the repeated measure. For the repeated measures ANOVA, islands were nested within locations (fringe vs. interior) and treated as experimental units. All effects were considered fixed, except for when testing for significant differences in habitat, which included location as a random effect to account for the nested structure of the sampling scheme. One-way ANOVAs were used to test for differences in soil

surface elevation among locations and habitats, and the interaction between them. Two-way ANOVAs were carried out for all leaf functional traits and nutrient concentrations, where comparisons were made across all habitat (i.e., edge and center) and season (i.e., wet and dry) combinations. Tukey HSD post-hoc tests were used to identify significant pairwise comparisons when ANOVAs indicated statistical differences. Repeated measures ANOVAs were performed using PROC MIXED (SAS Institute, Cary, NC, USA) and the one-way and two-way ANOVAs were performed in R v3.5.1 (R Core Team 2018).

We constructed linear mixed-effects models (with a Gaussian error distribution and identity link function) to address our research questions. Island habitat and season were included as fixed effects in the models to address questions 1 and 2, respectively, with water levels and porewater salinity being also included as the continuous covariates to parse out their marginal effects. We couple inference from these models to leaf nutrient analyses and our measurements of the hydrological environment to inform about nutrient and water use of *R. mangle* (question 3). Prior to model fitting, response variables were confirmed to meet the assumptions of data normality. Four separate models were constructed, one for each of four gas exchange variables of interest, A_{net}, g_{sw}, c_i, and *wue*. For each model, fixed effects for season (wet and dry), habitat (center and edge), porewater salinity and water level were considered, including interaction terms for water level and porewater salinity with season. In all models, random intercept terms were considered for location (i.e., fringe vs. interior), islands, and islands nested within location. Random slopes were explored but determined to not improve model fits. The best-fitting models were determined via stepwise model comparison using AIC based on backward selecting random effects then backward selecting fixed effects, as implemented with the 'lmerStep' function in the lmerTest R package (Kuznetsova et al. 2017). The best fitting models included a random intercept term for islands, which helped remove variability in the data because of the sampling design. Random effects for location (i.e. fringe vs. interior) were insignificant, signifying that most of the random variance in the gas exchange data was among islands, which we consider as the experimental unit in all mixed-effects models. The mixed effect models were fit using restricted maximum likelihood estimates via the lme4 R package (Bates et al. 2015). Models were evaluated using model predicting, tabling and plotting functions from the sjPlot R package (Lüdecke 2018). All analyses were complete in R v3.5.1 (R Core Team 2018).

RESULTS

Mangrove island micro-elevational differences and ecohydrology

Soil surface elevation significantly declined from mangrove island center to edge habitats from -0.14 ± 0.1 m at mangrove island centers to -0.4 ± 0.02 m at mangrove island edges, a mean difference of about 30 cm ($F_{1,20}$ = 108.42, p < .001; Table 1). Water levels relative to the soil surface were significantly higher in the edge than in center habitats ($F_{1,178}$ = 178.33, p < .001), measuring on average 36.9 ± 1.4 cm in edge habitats, and 12.8 ± 1.2 cm in mangrove island centers (Table 2). We recorded water levels of 0 cm (i.e., non-inundated habitats) in 10% of our measurements, and those were exclusive to mangrove island centers during the dry season. There was a significant effect of season ($F_{1,178}$ = 11.11, p < .001) on water levels, where they increased from 17.05 ± 1.5 cm in the dry season to 30.4 ± 1.6 cm in the wet season (Figure S1).

Continuous water level data recorded at the fringe and interior mangrove zones indicated a similar flooding trends between locations, with lower water levels during the dry season and higher water levels in the wet season, up to 40-47 cm above the soil surface in both locations (Figure S2). Water levels at the interior mangrove forest always remained higher than those registered in the fringe mangrove zone (Figure S2). Porewater salinity was significantly different between habitats ($F_{1,178}$ = 91.45, p < .001) and seasons ($F_{1,178}$ = 17.87, p < .001), with lower salinity values in the center (21.5 ± 0.3) of the islands relative to the edge (25.1 ± 0.3) habitats, and slightly lower porewater salinity during the dry season (22.5 ± 0.4) than in the wet season (24.1 ± 0.3; Table 2, Figure S1). There was no significant interaction ($F_{1,178}$ = 0.26, p > .05) between island habitats and seasons, indicating that the variation in porewater salinity between habitats is independent of seasonality (Table 2). Surface water salinity was not significantly different among center and edge habitats ($F_{1,163}$ = 2.36, p > .05), but increased significantly from the dry to the wet season ($F_{1,163}$ = 8.97, p < .01, Table 2). There was also a significant habitat-season interaction for surface water salinity, but a Tukey post-hoc HSD test indicated that only island center habitats in the dry season were different from all other pairwise comparisons (Table 2).

Rates of leaf gas exchange and their relationships to the hydrological environment

A_{net} measurements ranged from 0.1 to 15.1 µmol m^{-2} s^{-1}, with 90% of the observations recorded between 2 and 14 µmol m^{-2} s^{-1} (see Figure S3). g_{sw} values were low, ranging from <0.01 to 0.72 and averaging 0.1 mmol mol^{-1} (see Figure S3). Associated c_i values ranged from 40 to 377 and averaged 242 µmol mol^{-1}, with 98% of them being greater than 150 µmol mol^{-1}. Lastly, measured rates of *wue* varied between >0.01 and 0.21 mmol CO_2 mol H_2O^{-1}, being normally distributed about a mean value of 0.09 mmol mol^{-1}.

The linear mixed-effects model for A_{net} included fixed effects for island habitat, porewater salinity, water level, season, and an interaction term for water level with season (Figure S4 & Table S4). There was substantial variation in A_{net} rates among leaves (σ^2 of about 6 µmol m^{-2} s^{-1}), and the random variation among islands was about 0.02 µmol m^{-2} s^{-1} (see Table S4). All fixed effects were statistically significant ($p < .05$), except the interaction term, which was marginally significant ($p = .05$) but greatly improved model fit. Mangrove edge habitats reduced A_{net} by over 2.5 µmol m^{-2} s^{-1} relative to mangrove island centers (Figure 3). Seasonality had a comparable negative effect, leading to an average decrease in A_{net} of just over 2 µmol m^{-2} s^{-1} in the wet season relative to the dry season (Figure 3). After accounting for variation in the data because of habitat and season, the marginal effects of water level and porewater salinity were positive, albeit weak, leading to increases in A_{net} of <0.1 µmol m^{-2} s^{-1} per cm increase in water level (Figure 4) or per ppt increase in porewater salinity (Figure 5). Therefore, as water levels increased, A_{net} increased, with increases being consistent across habitats (Figure 4); a similar pattern was observed in relation to soil porewater salinity, although the magnitude of increase in A_{net} was smaller (Figure 5). These relationships of A_{net} with water level variability were consistent across seasons, although rates of A_{net} were depressed during the wet season (Figure 3). The mixed-effects model for A_{net} fit satisfactorily for these types of linear mixed effects models modeling leaf-gas exchange data using environmental predictors, explaining 24% of the variation in the data, 22% of which was explained by ecohydrological data (i.e., fixed effects) (Table S4).

g_{sw} was modeled using an identical mixed-effects model to that of A_{net} (Figure S5 & Table S5). Generally, rates of g_{sw} were low, with 98% of g_{sw} measurements being <0.2 mmol mol^{-1}. Random variance in g_{sw} among islands was negligible, being <0.01 mmol mol^{-1}. Leaf g_{sw} in edge habitats was statistically lower than that of mangrove island centers ($p < .001$), being depressed by about 0.02 mmol mol^{-1} (Figure 3). Water levels did not affect rates of g_{sw} ($p > .05$, Figure 4, Table S4), and soil porewater salinity had a marginal effect ($p = .07$) on g_{sw}, where conductance increased slightly at high salinities, after accounting for the effects of other environmental variables in the model (Figure 5). The effect of season on rates of g_{sw} was significant in the model, with the wet season leading to a 0.05 mmol mol^{-1} decrease in conductance (Figure 3) and the interaction between water levels and season being statistically significant (Figure 4). Overall, the mixed-effects model for g_{sw} did not fit the data as well as the model for A_{net}, in that the model only explained about 12% of the variability in the data, with 9% of its explanatory power coming from the environmental predictors (Table S5).

Although the model selection approach was the same as the other mixed-effects models, the best-fitting model for c_i was different from the models for A_{net} and g_{sw}. The model did not include a fixed effect for soil porewater salinity (which was dropped out of the model in the model selection procedure) but included all the same fixed effects as the models for A_{net} and g_{sw}, which were all statistically significant ($p < .001$), and a random intercept term for islands (Table S6). The fixed effect for porewater salinity was excluded from the best-fitting model because of limited variation in porewater salinity in the data set, and because the other factors (e.g., season) explained most of the variation in c_i over time. Island edge habitats had consistently higher c_i values than mangrove island centers, being about 27 µmol mol^{-1} greater (19 to 35, 95% CI; Figure 3). The marginal effect of season alone was similar in magnitude to that of habitat; the wet season led to a decrease in c_i of 24 µmol mol^{-1} (14 to 34, 95% CI) relative to the dry season (Figure 3, Table S6). Water levels, by themselves (again, the marginal effect), led to a slight decrease in c_i but had a positive interaction with season, indicating that the relative decrease in c_i due to increasing water levels was suppressed during the wet season (Figure 4). The random intercept term in the model (for islands) explained a considerable amount of variation in the data (σ^2 = 128 µmol mol^{-1}, with τ_{island} = 66 µmol mol^{-1}). The mixed-effect model for c_i fit the poorest of all four models, explaining just under 12% of the variance in c_i, about 9% of which was explained by data from the hydrological environment (Table S6).

Lastly, we modeled *wue* using a similar mixed-effects model to that of g_{sw}. As with the other linear mixed-effects models, the model included islands as a random effect. In the model for *wue*, all fixed effects were statistically significant ($p < .001$); however, the fixed effects were more subtle in magnitude. Similar to the model for c_i, porewater salinity was not included in the best-fitting model. *wue* values were normally distributed about a mean value of 0.09 µmol mol^{-1}, with 83% of the data having values between 0.05 and 0.15 µmol mol^{-1}. Mangrove island edge habitats had lower *wue* by 0.01 µmol mol^{-1} than island centers (Figure 3). The marginal effect of water level, although being statistically significant in the model, was negligible; however, the wet season caused an increase in *wue* by 0.02 µmol mol^{-1} relative to the dry season, with the interaction between water level and season being slightly negative (Figure 3, Figure 4). Random variation in *wue* structured across the eight mangrove islands measured was minuscule, being < 0.01 µmol mol^{-1}. The model fit for the *wue* mixed-effects model was comparable to and slightly better than the model for c_i, with fixed effects explaining just over 12% of the variance in the data, about 9% of which was explained using the environmental predictors (Table S7).

Rhizophora mangle leaf functional traits, nutrient content, and isotopic signatures

Leaf SLA values did not vary significantly between seasons ($F_{1,155}$ = 0.46, p > .05) and island habitats ($F_{1,155}$ = 3.07, p > .05, Table 2), demonstrating that leaves were morphologically equivalent, despite having some variation in SLA with average values ranging from 29 to 40 g cm^{-2}. Similarly, leaf water content was not significantly different between all season-habitat combinations ($F_{1,155}$ = 0.32, p > .05), despite a statistically significant effect of season alone ($F_{1,155}$ = 9.10, p < .01), where leaf water content was greater in the dry season (65.6 ± 0.3%) relative to the wet season (63.8 ± 0.4%, Table 2).

Leaf TC content ranged from 400 to 450 mg g^{-1} (Table 3) and was not different between seasons ($F_{1,155}$ = 1.10, p > .05), habitat ($F_{1,12}$ = 0.10, ns), or their interaction ($F_{1,12}$ = 1.77, p > .05). Leaf TN concentrations were higher in the dry season compared to the wet season ($F_{1,12}$ = 11.95, p < .01) and ranged from 8-10 mg g^{-1} (Table 3). There was no significant difference ($F_{1,12}$ = 11.86, p > .05) in leaf TN between habitats nor a significant interaction ($F_{1,12}$ = 0.11, ns) between seasons and habitats (Table 3). Leaf TP content did vary between seasons ($F_{1,28}$ = 22.89, p < .001) and habitats ($F_{1,28}$ = 8.97, p > .05), but the interaction effect was not significant ($F_{1,28}$ = 0.002, ns). Mean leaf TP values ranged from 0.43 to 0.56 mg g^{-1} across seasons and habitats, with higher concentrations during the dry season than in the wet season and higher leaf tissue TP values in the island center habitats compared to edge habitats (Table 3). Mean N resorption for *R. mangle* leaves was slightly similar across seasons and habitats and ranged from 60 to 63% (Table 3). P resorption of leaf tissue had a broad range compared to that of N, ranging from 73.2 ± 6.2% (center, wet season) to 78.6 ± 0.2% (edge, dry season) across seasons and habitats. Overall, P resorption of *R. mangle* leaves was higher in the edge habitats relative to the center during both seasons (Table 3).

Patterns in green leaf carbon isotope signatures ($\delta^{13}C$) mirrored those of leaf TN and TP concentrations. Carbon isotopic fractionation was more negative during the wet season than in the dry season ($F_{1,12}$ = 18.88, p < .01, Table 3, Figure 6), with no statistical difference between habitats ($F_{1,12}$ = 1.17, p > .05). Green leaves bulk $\delta^{13}C$ values ranged from -25.9 to -25.1‰ across seasons and habitats (Table 2). Physiologically, the differences in carbon isotopic fractionation were estimated to result in a maximum difference of about 10 µmol mol^{-1} c_i between the center and edge habitats and a difference of 5 to 15 µmol mol^{-1} c_i within habitats ($F_{1,12}$ = 1.71, p > .05) because of seasonality ($F_{1,12}$ = 18.88, p < .01). These differences resulted in greater c_i in mangrove island centers than in edge habitats (i.e., the interaction between season and habitat marginally significant ($F_{1,12}$ = 4.53, p = .055, Table 3). Intrinsic water-use

efficiency (*WUE*) was calculated from leaf $\delta^{13}C$ values; accordingly, *WUE* was greatest in mangrove island centers during the dry season relative to all habitat-season combinations. Additionally, *WUE* was significantly lower in the wet season than the dry season ($F_{1,12}$ = 18.88, p < .01, Table 3). Mean leaf bulk $\delta^{15}N$ values were significantly ($F_{1,12}$ = 19.66, p < .001) higher in the center habitats (-0.60 ± 0.66‰) relative to the edge (-4.79 ± 0.66‰), but there was no difference between seasons ($F_{1,12}$ = 0.17, ns) and no interaction between season and island habitat ($F_{1,12}$ = 0.58, ns, Figure 6A, Table 3).

DISCUSSION

Leaf form and leaf tissue nutrient concentrations

We consistently measured leaves at the second-most terminal leaf pair on the leaf rosette and found a comparable range in SLA values, from about 29 to 40 $cm^2\ g^{-1}$ (Table 2). SLA of leaves of *R. mangle* trees in full sun in coastal Belize ranged from 30.4 to 56.1 $cm^2\ g^{-1}$, increasing toward the terminal end of leaf rosettes (i.e., with decreasing leaf age) (Farnsworth and Ellison 1996). There were no statistical differences in the SLA of any of the leaves we collected, over time, among islands or between habitats. Moreover, all leaves had comparable leaf dry masses and leaf water contents (Table 2). Thus, we have confidence that all of the leaves this study measured for leaf gas exchange and used in nutrient analyses are functionally comparable. Leaf carbon content was not different among leaves, measuring between 37.7 and 46.3 %, which is consistent with leaf carbon content of *R. mangle* leaves from trees in the Guaratiba Reserve near Rio de Jainero, Brazil (Rodrigues et al. 2015), and potentially globally.

We measured leaf N concentrations between 8 and 10 mg g^{-1}, which were slightly greater in the dry season than in the wet season and slightly greater in center than edge mangrove island habitats. Differences in Leaf N were only statistically higher between the center habitat in the dry season than in the edge habitat in the wet season (Table 3), pointing to a potential habitat-season interaction on variation in leaf N. Leaf P contents were less than 0.63 mg g^{-1}, averaging 0.48 mg g^{-1}; which is very low, considering that leaf P for tropical trees averages about 1.4 mg g^{-1} in the TRY database (n = 2962; Kattge et al. 2020). Leaf P concentrations were lower in the wet than the dry season and lower in the edge habitat than in mangrove island centers (Table 3), suggesting that freshwater inputs affect P sorption in the soils, uptake by roots, and mangrove whole-plant and leaf P status, even at seasonal timescales. Typically, leaf tissue N:P ratios >20 indicate P-limitation (Güsewell 2004), although for wetland ecosystems, P-limitation may occur at N:P ratios close to 25 (Wassen et al. 1995). We measured leaf N:P ratios, which all averaged >40, confirming strong *R. mangle* leaf tissue

P-limitation at TS/Ph-7. These results are also consistent with high N:P ratios (126) measured in root tissues at this site (Castañeda-Moya et al. 2011), underscoring the strong P limitation condition of scrub mangroves in Taylor River.

Seasonal signals in R. mangle *physiology with implications for ecosystem functioning*

Because data were conveniently grouped by season to account for how precipitation, temperature and other environmental drivers might affect *R. mangle* gas exchange at TS/Ph-7 throughout the calendar year, we must first discuss the effect of season before going on to discuss the effects of habitat or water levels and salinity. A_{net} varied over 2.5 µmol m^{-2} s^{-1}, and g_{sw} varied about 0.25 mol m^{-2} s^{-1} within habitats between the wet and dry seasons (Figure 3). Despite differences in A_{net} and g_{sw} between seasons, we found no statistical differences in c_i and *wue* between seasons, although there was some variation (Figure 3). This points to habitat-specific optimization of the diffusion of CO_2 into (i.e., c_i) and the movement of water vapor out of (i.e., *wue*) leaves (Cardona-Olarte et al. 2006, Barr et al. 2009, Reef and Lovelock 2015, Lopes et al. 2019). As precipitation and freshwater flow increased during the wet season, water levels rose, and mangrove island centers experienced greater inundation levels (Figures S1 & S2), resulting in decreased A_{net} and g_{sw} (Figure 3). A similar reduction in A_{net} and g_{sw} was measured in mangrove island edge habitats during the wet season (Figures 3 & 4). Although A_{net} was depressed in the wet season, the effect of inundation levels on reducing A_{net} was consistent across seasons (Figure 4). g_{sw} showed a similar pattern to A_{net}, being highest in mangrove island centers during the dry season (Figure 3). The effect of water levels on g_{sw}, however, resulted in increased g_{sw} in the wet season, an effect which was tempered during the dry season (Figure 4).

In the Florida Everglades, irradiance peaks in at the April and May (Barr et al. 2009), and rainfall and temperature reach maxima in June, July, and August (Figure 1 A, B). Thus, photosynthetic demand for water is likely highest at the end of the dry season in April and May. During this time, we measured lower water levels and porewater salinity levels relative to the wet season. Barr et al. (2009) recorded earlier diurnal and more considerable reductions in g_{sw} during late May versus July or August for mangroves at Key Largo. Additionally, greatest A_{net} rates for tall fringe mangroves in the southeastern Everglades occur from March to May (Barr et al. 2009). The difference in surface water and porewater salinity (*Δsw-pw*) can be used as a proxy for tree transpiration. Average *Δsw-pw* measured 10.7 and 8.1 ppt at mangrove island edges in the wet and dry seasons, respectively, whereas, it measured 7.8 and -0.3 in mangrove island centers in the wet and dry seasons, respectively. Indeed, photosynthetic transpiration

was highest in March and April (Figure S3). Thus, photosynthetic demand for water is higher in the dry season in mangrove island centers relative to edges or either habitat in the wet season. The drying of the soils at slightly higher elevation island center habitats in this scrub mangrove forests likely increases A_{net}. Thus, the seasonal variation in hydrology, mainly reductions in water levels and porewater salinity during the dry season, albeit coupled with an increase in surface water salinity in this study (Table 2), likely have key consequences for mangrove forest carbon fluxes at greater spatial scales. Potentially drying of soils could also lead to an increase in ecosystem respiration (Chambers et al. 2014). As such, future research could look at soil metabolic dynamics (e.g., soil respiration, microbial C and N, or changes in microbial communities) with hydrology and season, which may show unique responses in this scrub *R. mangle* forest (Lovelock 2008, Chambers et al. 2014)

The effect of mangrove island habitat on leaf gas exchange

Our results showed significant differences in soil elevation between mangrove island habitats (Table 1), which had an apparent effect on *R. mangle* leaf gas exchange rates (Figures 3, 4, 5). Changes in root biomass and productivity between the center and edge island habitats drive the elevation gradient within islands because of differences in soil depth (Table 1). Overall, higher total (0-90 cm depth) root biomass (5975 ± 1333 g m^{-2}) and productivity (491 ± 64 g m^{-2} y^{-1}) are observed in the center habitat compared to the edge (3379 ± 638 g m^{-2} and 323 ± 18 g m^{-2} y^{-1}, respectively – Castañeda-Moya et al. 2011). With elevational differences of approximately 0.3 meters between mangrove island center and edge habitats, we measured clear differences in A_{net} and g_{sw} (Figure 3). A_{net} was nearly 3 µmol m^{-2} s^{-1} greater at mangrove island centers than edges, and g_{sw} was >1 mol m^{-2} s^{-1} higher; these differences were attributable to mangrove island habitat alone, after accounting for variation explained by water level, salinity or seasonality (i.e., they are marginal differences). Associated c_i concentrations were about 30 µmol mol^{-1} lower and *wue* was >0.01 mmol mol^{-1} greater at island centers than at island edges (Figure 3).

Thus, these findings support our first hypothesis about the effect of habitat micro-elevation (center vs. edge) on A_{net}, with overall greater leaf gas exchange rates at mangrove island centers compared to their edges. Interestingly, the effect of habitat on *R. mangle* leaf gas exchange rates was similar in magnitude to the effect of season (Figure 3). The magnitude of variation in A_{net} that we report in this study is slightly larger than the magnitude of variation reported by Lin and Sternberg (1992) who found that A_{net} varied up to 2 µmol m^{-2} s^{-1} between scrub and fringe *R. mangle* trees in the nearby Florida keys. Furthermore, our A_{net}

measurements with average values between 5.7 µmol m^{-2} s^{-1} (edge habitat, wet season) and 10.2 µmol m^{-2} s^{-1} (center habitat, dry season, Figure 3), are within the range of values reported for *R. mangle* interior scrub (5.3 µmol m^{-2} s^{-1}) and fringe (10 µmol m^{-2} s^{-1}) mangroves along a distinct zonation pattern in the intertidal zone in Twin Cays, Belize (Cheeseman and Lovelock 2004). These results demonstrate the effect that higher elevation center habitats at TS/Ph-7 have on alleviating inundation stress, which pervades scrub mangrove physiology, making trees growing in center habitats in the dry season physiologically comparable to tall, fringe mangroves. Certainly, the stress relief is short lived when water levels rise in the wet season (Table 2, Figure S1), and rates of leaf gas exchange are depressed once more (Figure 3).

The effect of water level and salinity on R. mangle *leaf gas exchange*

During 2019, the hydrological environment (Figure 1C,D) at our study site was seasonally dynamic (Table 1) and tended to mirror patterns in local rainfall (Figure 1B) in a manner consistent with our understanding of climate of the region (Abiy et al. 2019). Water level and porewater salinity both increased during the wet season (Table 2, Figure S1) from the beginning of the rainy season in May through November. This likely led to increased water column stratification via an increase in the freshwater lens (Hughes et al. 1998, Uncles et al. 1992). Indeed, the difference in surface water and porewater salinity increased in the wet season, with surface water salinities decreasing, despite a slight increase in porewater salinities (Table 1). When data were grouped by season, edge habitats were slightly more saline (about 4 ppt on average) than mangrove edges (Table 1), and there were no clear differences between fringe and interior scrub mangrove zones (Figures S1 & S2).

Rates of mangrove leaf gas exchange (i.e., A_{net} and g_{sw}) typically decrease with porewater salinity, especially along strong salinity gradients in the environment (i.e., gradients >30 ppt, Ball 2009, Clough and Sim 1989, Lugo et al. 2007). Porewater salinity was only included in the linear mixed-effects models for A_{net} and g_{sw}, and its effect was minimal, reducing A_{net} by <1 µmol m^{-2} s^{-1} per ppt increase in porewater salinity and not affecting g_{sw}. Like the effect of porewater salinity on A_{net}, the effect of porewater salinity on g_{sw} was small in magnitude and consistent across seasons and mangrove island habitats (Figure 5). The minimal influence of porewater salinity on leaf gas exchange is likely due to the small seasonal and spatial variations that we observed between fringe and interior mangrove zones. Differences were not large, maximizing at 16.4 ppt and averaging 5.2 ppt, especially when considering that *R. mangle* frequently occupies natural habitats that have salinities greater than seawater (Reef and Lovelock 2015), potentially up to 50-60 ppt (Cintron et al. 1978). At our

study site, variation in porewater salinity from long-term monitoring data (2001-2020) have shown similar magnitudes of relatively minor variation in porewater salinity, with overall mean values ranging from 19-22, and rarely exceeding 30 ppt (Castañeda-Moya et al. 2013). Indeed, long-term variation in porewater salinity (<30 ppt) across the FCE mangrove sites (Shark and Taylor River sites) are below the critical value (65 ppt) that influences forest structure and productivity across the FCE landscape (Castañeda-Moya et al. 2013). Thus, the limited effects of salinity in the linear mixed effects models, using data from the 2019 calendar year are likely broadly applicable in space and time across scrub *R. mangle* forests of the southwestern Everglades.

The effects of inundation on *R. mangle* photosynthesis can be difficult to separate from the effects of salinity, however the linear mixed modeling approach we used permitted doing so. In typical greenhouse experiments where mangrove seedlings are grown, inundation alone has little effect on several *Rhizophora* species photosynthesis or biomass production (Pezeshki et al. 1990b, Hoppe-Speer et al. 2011). Inundation may sometimes lead to increases in rates of leaf gas exchange over the short term, and often interacts with salinity over time to reduce A_{net}, g_{sw} and growth rates (e.g., Cardona-Olarte et al. 2013). Thus, water levels and flooding duration are key drivers controlling A_{net} in mangroves. For instance, findings from a long-term greenhouse inundation study by Farnsworth and Ellison (1996) exemplify how short-term responses of *R. mangle* to inundation differ from longer-term responses. Over several years, high inundation levels led to steady declines in A_{net} of up 25% for a given g_{sw} and decreases in growth rates. Results of the high water level (30-40 cm above soil surface) treatment were similar to those of the low water level (10-15 cm) treatments, suggesting that *R. mangle* physiology is optimized at inundation levels that reach just a few centimeters above the soil surface at high water level (Ellison and Farnsworth 1997). Indeed, we found that the intermittent flooding conditions of mangrove island centers that averaged water levels, or 10-15 cm above the soil surface, allowed greater A_{net} and g_{sw} than permanently flooded mangrove island edges, which averaged water levels of 30-40 cm. Thus, the water level regime in center habitats allows for mangrove soils to repeatedly flood and desiccate, which may help the species to maintain optimal stem water potentials and g_{sw} (Ball 2009, Reef and Lovelock 2015).

Although initial increases in *R. mangle* g_{sw} can result from short term inundation (Krauss et al. 2006, Hoope-Speer et al. 2011), especially at low salinities (Pezeshki et al. 1990b), several studies have linked stomatal closure to longer-term inundation (Kozlowski 1997, Ellison and Farnsworth 1997, Huang 2000). We measured depressed g_{sw} during the wet season and in

677 mangrove island edge habitats relative to centers, an effect that was not attributable to water
678 levels, after accounting for variation in seasonality and habitat. Our measurements of g_{sw} were
679 consistent with those reported in other studies from across a range of inundation levels (Clough
680 and Sim 1989, Lin and Sternberg 1992, Ellison and Farnsworth 1997, Krauss et al. 2006, Lugo
681 et al. 2007, Barr et al. 2009), supporting the understanding that *R. mangle* leaves limit g_{sw} in
682 response to flooding to optimize c_i for carbon gain without losing unnecessary amounts of water.
683 Indeed, Ball and Farquhar (1984) reported c_i values of around 170 µmol mol^{-1}in Australian
684 mangroves, where c_a (the concentration of extracellular CO_2) was roughly twice that of c_i.
685 Correcting these values to atmospheric CO_2 concentrations in 2019 (i.e., 408 µmol mol^{-1}) yields
686 c_i values of 247 µmol mol^{-1}, which is within the range of c_i values measured at the center and
687 edge mangrove habitats in our study site (range = 220-260 µmol mol^{-1}).

688 Rhizophora mangle *CO_2 assimilation and stomatal behavior*

689 The A_{net}-c_i relationship for *R. mangle* (Figure S8) and other salt-tolerant wetland plants
690 warrants discussion because it results in unusual stomatal behavior (i.e., explains low rates of
691 g_{sw}, Ball 2009). To understand this relationship, we must realize how salinity affects A_{net} in
692 relation to g_{sw}. Increasing salinity results in a downward translation of the A_{net}-c_i curve (i.e.,
693 lowers A_{max}) and a decline in the initial slope of the A_{net}-c_i relationship (i.e., a proportional
694 reduction in A_{net} per µmol mol^{-1} increase in c_i) (see Figure 3 in Ball 2009, taken from Ball and
695 Farquar 1984). Additionally, mangrove leaves almost always function at low g_{sw} (i.e., typically
696 <0.25 mol m^{-2} s^{-1} and "with an operational c_i in the transition region of the A-ci curve," *sensu* Ball
697 2009) with c_i values of <200 µmol mol^{-1} (as reported by Ball 2009) to limit water loss relative to
698 carbon gain and to maximize *wue.* Ball (2009) describes two hypothetical scenarios that typify
699 changes in the A_{net}-c_i relationship for mangroves. The first assumes no change in the leaf's
700 photosynthetic potential (i.e., no change in the A_{net}-c_i characteristics), which results in a
701 decrease in c_i and an increase in *wue* when stomates close at the expense of A_{net}. The second
702 scenario occurs when the photosynthetic potential of the leaf increases in concert with stomatal
703 closure (i.e., a decrease in g_{sw}), which results in a similar decrease in c_i and an increase in *wue*,
704 however at the expense of leaf nitrogen because of the increase in the photosynthetic
705 machinery per unit leaf area. We observed differences in leaf nitrogen content that reflect
706 differences in A_{net} (Table 2). Thus, variation in c_i and *wue* reflect differences in the
707 photosynthetic capacity of leaves among mangrove island habitats. Moreover, because
708 mangroves are particular in the degree to which they open their stomata in order to limit water
709 loss, the differences in g_{sw} between center and edge mangroves habitats are likely a function of

inherent differences in the photosynthetic capacities of the leaves of mangrove trees in those respective habitats. Such differences might be attributable to differences in the acclimation of leaves to light intensity or because of inundation stress (e.g., lower rates of nutrient acquisition or sapflow), and may result from an interaction between light and flooding to optimally tune photosynthetic potential as a strategy of coping with inundation stress .

R. mangle *water use at TS/Ph-7*

Leaf carbon isotopic $\delta^{13}C$ fractionation values reflect g_{sw} integrated over leaf lifespan. Rubisco, the photosynthetic enzyme, discriminates against the heaver $\delta^{13}C$ (O'Leary 1988, Farquhar et al. 1989), which occurs naturally in the atmosphere at roughly -8.5‰ and has been trending more negative as the anthropogenic impact on the atmosphere intensifies (Dlugokencky and Tans 2020). Thus, $\delta^{13}C$ values more negative than -8.5‰ in leaf tissues indicate a longer residence time of air (i.e., CO_2) in leaf intracellular air spaces, and thus lower g_{sw} (Marshall et al. 2007, Lambers et al. 2008). We found *R. mangle* leaf $\delta^{13}C$ fractionation values between -25 and -26‰, which were slightly more negative in the wet season relative to the dry season. The seasonal differences in leaf $\delta^{13}C$ fractionation were greater in magnitude for island center habitats than for edge habitats, although not statistically significant (Figure 6, Table 2). Our $\delta^{13}C$ values are consistent with previously reported values for *R. mangle* leaves at our study site during 2001, with a bulk $\delta^{13}C$ mean value of -26.4‰ (Mancera-Pineda et al. 2009). Medina et al. (2010) reported leaf $\delta^{13}C$ values between -23 and -27‰ along a fringe-inland mangrove transect in eastern Puerto Rico, with carbon isotopic fraction being more-negative at the interior scrub mangrove zone relative to the fringe zone, which is dominated by taller (~4 m) mangroves. Patterns in isotopic signatures in their study were associated with a combination of P-limitation and seasonal water stress, similar to the environmental conditions present at our scrub mangrove site (Mancera-Pineda et al. 2009, Castañeda-Moya et al. 2011, 2013). Likewise, the positive linear relationship between salinity and *R. mangle* foliar $\delta^{13}C$ values along Shark River estuary in the southwestern Everglades with more enriched values in upstream (-27.8‰) estuarine regions relative to the estuary mouth (-32.3‰) (He et al. 2020), indicates how increases in salinity along an estuarine gradient decrease foliar bulk $\delta^{13}C$ values.

We can compare instantaneous water use efficiency (*wue*) measured using our portable gas exchange system with intrinsic water use efficiency from leaf carbon isotopes (*WUE*). Both metrics were similar in range, with concordant indications that water-use efficiency in mangrove island centers during the wet season is about 0.1 mmol mol^{-1} (Figure 3, Table 2). *WUE* was not different between habitats during the wet season (Table 2), but *wue* was lower at edges than

743 their centers during the wet season (Figure 3). *WUE* increased in dry season relative to the wet
744 season, with differences between habitats emerging during the dry season (Table 2); whereas
745 *wue* was not different among seasons but showed consistent differences between mangrove
746 island center and edge habitats (Figure 3). However, the linear mixed-effects model for *wue*
747 attributed some of the variation in the data to fluctuations in water levels (Figure 4), showing that
748 *wue* increases when water levels are higher, and that this increase is more significant in the dry
749 season relative to the wet season. Therefore, water levels are related to *R. mangle* water use
750 efficiency.

751 Comparing our calculations of *wue* to those of other studies shows that the scrub *R.*
752 *mangle* trees at TS/Ph-7 are toward the higher end of the range of *wue* for the species, which
753 ranges from 0.1 to 0.9 mmol mol^{-1} (see Table 2 in Barr et al. 2014). Soares et al. (2015)
754 reported a similar range (0.2 to 0.8 mmol mol^{-1}) in *wue* for in mixed mangrove forests in three
755 estuaries along the Santa Catarina State in southeastern Brazil. In contrast, lower *wue* rates
756 (0.042 mmol mol^{-1}) have been reported for adult *R. mangle* plants growing naturally in the field
757 under seawater (35 ppt) conditions in a Venezuelan mangrove forest (Sobrado 2000). Studies
758 have demonstrated that *wue* increases with salinity in Old World *Rhizophora* trees, ranging from
759 0.35 to 0.8 mmol mol^{-1} (Clough and Sim, 1989). Similarly, Lopes et al. (2019) measured greater
760 *wue* at higher salinities but a more significant seasonal variation in *wue* for lower salinity areas
761 in riverine mangroves of the São Mateus River in southeastern Brazil. Our results indicate little
762 effect of porewater salinity on the *wue* of scrub *R. mangle* leaves at TS/Ph-7, which is likely due
763 to the small variation in porewater salinity measured at the site (as discussed above).

764 R. mangle *nutrient use at TS/Ph-7*

765 Resorption, of nutrients from senescent leaves prior to leaf fall is a within-stand nutrient
766 recycling mechanism that may reduce nutrient losses via tidal export in coastal systems
767 (Vitousek 1982, Aerts and Chapin 2002). Like other tropical trees, mangroves exhibit several
768 physiological mechanisms that reduce nutrient losses via tidal exchange, including resorption of
769 N and P prior to leaf abscission (Twilley et al. 1986, Alongi et al. 1992). Increased availability of
770 a limiting nutrient can change nutrient use and conservation patterns in mangroves (Feller et al.
771 2003a, 2003b). For instance, N resorption efficiency of *R. mangle* trees increased in response
772 to P addition in the scrub mangrove zone at Twin Cays, Belize; however, the addition of N had
773 no effect on either N or P resorption efficiencies of scrub mangroves (Feller et al. 2003a). We
774 found little variation (60-63%) in N resorption efficiencies for *R. mangle* leaves across scrub
775 mangrove island habitats. In contrast, higher overall efficiencies of P resorption (73-79%) of

776 leaf tissue were measured across habitats, with higher P resorption in mangrove island edge
777 habitats relative to centers. These results suggest that *R. mangle* conserves P better than N in
778 this P-limited environment. Our findings are roughly comparable to N and P resorption
779 efficiencies for *R. mangle* in the control plots of scrub-dominated forests in Panama (~50%, and
780 80%, respectively; Lovelock et al. 2004).

781 Mangrove species prioritize resorption of nutrients that are limited in the soil. It has been
782 suggested that plants growing in nutrient-poor environments resorb a higher proportion of
783 nutrients, potentially decreasing nutrient loss by efficient nutrient recycling (Chapin and
784 Moilanen 1991). Our findings support this understanding and indicate that the canopy N and P
785 resorption efficiency at TS/Ph-7 potentially results from the differential partitioning of these
786 nutrients among leaf stages and within the soil. Low soil TP concentrations probably determine
787 the higher recycling efficiency of P relative to N. Indeed, soil (0-45 cm depth) TP concentrations
788 in mangrove soils at TS/Ph-7 (0.06 ± 0.004 mg cm^{-3}) are three times lower than soils at the
789 mouth of Shark River estuary (SRS-6) dominated by fertile well-developed tall riverine
790 mangroves, resulting in extreme P limitation with average soil N:P ratios of 102 ± 6 (Castañeda-
791 Moya et al. 2013). Therefore, the non-homogeneous distribution of essential nutrients within
792 mangrove habitats creates distinct gradients and hot spots along the intertidal zone, influencing
793 the efficiency of internal nutrient recycling, as has been observed in other mangrove studies
794 (Feller et al. 2003a). This is supported by observations that nutrient resorption efficiencies in
795 mangroves vary with nutrient availability, e.g., via nutrient addition (Feller et al. 1999, Feller et al.
796 2003b) or along natural fertility gradients (Medina et al. 2010). Such variation in nutrient
797 availability and resorption efficiencies within mangrove trees likely scales with variation in
798 productivity (e.g., litterfall) and carbon residence times (e.g., soil and biomass dynamics) of
799 mangrove forests.

800 Foliar $\delta^{15}N$ values integrate long-term processes of N sources because isotopic
801 fractionation against the heavier isotope (i.e., ^{15}N) occurs during N transformations and
802 interactions between biotic (e.g., mycorrhizal fungi, or bacteria) and biogeochemical (e.g.,
803 nitrification, denitrification) nutrient cycling processes (Garten 1993). In our study site, patterns
804 of $\delta^{15}N$ in *R. mangle* leaves differed drastically between mangrove habitats, with values around
805 -4 to -5‰ for mangrove edge habitats and between 0 and -1‰ for island centers, indicating
806 lower ^{15}N discrimination in island center habitats (Table 2, Figure 6A). These $\delta^{15}N$ values are
807 considerably more depleted than the *R. mangle* leaf $\delta^{15}N$ values reported for riverine
808 mangroves along Shark River estuary (He et al. 2020), where values were negatively correlated

with distance inland from the mouth of the estuary, with more enriched leaves occurring near the mouth of Shark River (4‰) relative to upstream (0.4‰) regions. Reported $\delta^{15}N$ values for *R. mangle* leaves across different ecotypes in the neotropics range from 0 to -11‰, with more negative values for scrub mangrove forests (-5 to -10‰) than for fringe mangroves (0-7‰; Reis et al. 2017a). Similarly, a recent study showed that leaves from interior scrub mangrove communities had more negative $\delta^{15}N$ values than tall fringe mangroves in eastern Puerto Rico (-12‰ vs. 0‰, respectively; Medina et al. 2010). Those $\delta^{15}N$ values were more negative than those reported for scrub *R. mangle* forests in Florida (Fry et al. 2000), Belize (McKee et al. 2002, Wooller et al. 2003, Fogel et al. 2008), or Brazil (Reis et al. 2017b).

Patterns of foliar $\delta^{15}N$ between mangrove ecotypes can be discerned using *in situ* leaf nutrient content. Indeed, a direct relationship between ^{15}N discrimination and leaf N:P ratios of *R. mangle* leaves previously reported for the six FCE mangrove sites, including our study site, indicates that leaf N:P ratios accounted for 70% of the variability in ^{15}N discrimination (Mancera Pineda et al. 2009). Thus, foliar ^{15}N composition can reflect *in situ* N status and differences in plant N use. Hypoxic conditions in the soil may inhibit denitrification and ammonia volatilization, two processes that enrich the soil substrate in ^{15}N (Craine et al. 2015). Therefore, the substrate should be less enriched at the edge relative to the center, because of interactions with the soil and the open water can alleviate hypoxia. Thus, it appears that more negative $\delta^{15}N$ values in the edge habitats may be associated with lower inorganic N (i.e., ammonium) use by edge mangrove trees compared to those in center island habitats (Fry et al. 2000). Another potential explanation of why $\delta^{15}N$ values were more negative at mangrove island edges than in their centers is because lateral surface roots of *R. mangle* can extend into open water where they associate with symbiotic biofilms (i.e., algae and aquatic bacteria) that facilitate N acquisition from open water (Potts 1979). A significant source of isotopic discrimination occurs during N transfer between belowground symbionts (e.g., mycorrhizal fungi or bacteria) and plant roots during processes such as nitrification, denitrification, and ammonia volatilization. The lighter isotope ^{14}N reacts faster than ^{15}N (i.e., is preferentially given to the host plant by the symbiont), so that plant tissues are depleted, while substrates are enriched (Högberg 1997, Robinson 2001). Indeed, at our study site, we have observed several long, absorptive, fine lateral root systems that protrude from the edge of mangrove islands into the open water where biofilms colonize them.

Mangrove trees can potentially adapt to nutrient shortage or localized nutrient deficiencies in the soil by altering root system architecture and morphology and thus, patterns of

842 nutrient use. This plant strategy may maximize the efficiency of capturing limiting resources
843 essential for growth (e.g., N, P) from soil or surrounding open water areas in nutrient-poor
844 environments such as Taylor River, as proposed by the optimal plant allocation theory (Chapin
845 et al. 1987, Gleeson and Tilman 1992). We observed a slight decrease in foliar $\delta^{15}N$ during the
846 wet season (Figure 6A, Table 3), as water levels and porewater salinity increased, suggesting
847 that N-acquisition by *R. mangle* via algal biofilms may be slightly greater in the dry season than
848 in the wet season. Our results contrast with those of Mancera-Pineda et al. (2009), who
849 reported mean $\delta^{15}N$ values of +3 from 65 mature leaves collected in 2001 at our study site. We
850 argue that differences in $\delta^{15}N$ values between the two studies could be attributed to the location
851 where leaves were collected during the 2009 study, concluding that it is very likely that
852 Mancera-Pineda et al. only collected leaves from the center of mangrove islands, avoiding edge
853 habitats. Taking this into consideration, mangrove island centers potentially have even more
854 positive $\delta^{15}N$ signatures than we found, illustrating that in the center of mangrove islands, N is
855 taken up by roots in inorganic soluble forms (e.g., porewater ammonium, nitrate) readily
856 available for plant uptake, and not biotically via root symbionts. Lastly, highly depleted (i.e.,
857 negative) N isotopic values in leaf tissues is characteristic of tropical wetlands with P limitation
858 because P-limitation increases N fractionation, especially in flooded wetlands with limited P
859 pedogenesis (McKee et al. 2002, Troxler 2007, Medina et al. 2008), as is the case with the
860 scrub *R. mangle* forest at TS/Ph-7 where the main source of P is the ocean (Childers et al 2006).
861 Soil total P concentrations in top 10 cm of the peat soils at this site have measured 0.055 (±
862 0.01) mg cm^{-3}, with atomic N:P ratios of roughly 72 (± 2) (Mancera-Pineda et al 2009), which is
863 considerably lower than soils of most mangrove forests globally, but consistent with mangrove
864 forests in karstic environments (Rovai et al 2018).

865 **CONCLUSIONS**

866 In summary, habitat heterogeneity, resulting from micro-elevational differences in
867 mangrove tree locations on islands within the open water-mangrove island forest landscape,
868 drives variation in *R. mangle* leaf physiological performance. Mangrove island edge habitats
869 experience greater and more-prolonged inundation than island centers in a seasonal dynamic,
870 which leads to reductions in g_{sw}, reduced A_{net}, and lower photosynthetic *wue*. Conversely,
871 mangrove island center habitats are alleviated from inundation stress in the dry season, leading
872 to increases in A_{net} and g_{sw}. Interestingly, c_i levels increase with increasing water levels
873 because inundation likely slows not only g_{sw}, but the entire biochemical process of CO_2
874 assimilation, including mesophyll and lower level (i.e., cell wall, plasma membrane, cytosol)

conductance. Reductions in A_{net} interact with the salinity of the water that inundates scrub *R. mangle* trees, in theory, because g_{sw} rates are low and primarily respond to water loss from leaves rather than carbon gain. Additionally, differences in nutrient (i.e., N) acquisition and use patterns among scrub *R. mangle* trees growing at island edges vs. centers affect leaf nutrient status and photosynthetic potential.

Therefore, the interaction of inundation stress with mangrove island micro-elevational habitat principally alters tree water and nutrient use dynamics, which appear to cascade to affect leaf gas exchange rates through their effects on g_{sw}. Predominantly, prolonged inundation more than porewater salinity showed this effect in our measurements at TS/Ph-7 because the hydrological regime in Everglades mangrove forests is characterized by distinct hydroperiod regimes across the coastal landscape, with long hydroperiods and minor fluctuations in salinity throughout the year (Figure S2). At the forest level, such physiological differences in scrub mangrove functioning with habitat and the hydrological environment can help to parameterize demographic and carbon flux models to forecast ecosystem trajectories in response to the impacts of sea-level rise and saltwater intrusion in this coastal region. This is particularly significant given the current freshwater restoration efforts in the Everglades and the associated uncertainties of water management on the spatial distribution of mangrove forests in the Everglades landscape with projected climate change scenarios.

ACKNOWLEDGEMENTS

This research was supported by the Department of Interior – National Park Service (Cooperative Agreement #P16AC00032) and the Florida Coastal Everglades Long-Term Ecological Research (FCE-LTER) program funded by the National Science Foundation (Grant #DEB-1832229). We thank Mandy Kuhn, Austin Pezoldt, and Ralph Diaz-Hung for field assistance. We thank the Everglades National Park for granting research permits and the Florida Bay Interagency Science Center-Everglades National Park (FBISC-ENP) for logistic support during the study. We thank Dr. Zoran Bursac from the center for Statistical Consulting and Collaboration at FIU for statistical advice. We thank Prof. Ernesto Medina and two anonymous reviewers for constructive comments on an earlier version of this manuscript. This is contribution number XX from the Southeast Environmental Research Center in the Institute of Environment at Florida International University.

REFERENCES

Abiy AZ, Melesse AM, Abtew W, Whitman D (2019) Rainfall trend and variability in Southeast Florida: Implications for freshwater availability in the Everglades. PLoS One 14:e0212008.

Adame MF, Kauffman JB, Medina I, Gamboa JN, Torres O, Caamal JP, Reza M, Herrera-Silveira JA (2013) Carbon stocks of tropical coastal wetlands within the karstic landscape of the Mexican Caribbean. PLoS One 8:e56569.

Aerts R, Chapin FS. (2002) The mineral nutrition of wild plants revisited: a re-evaluation of processes and patterns. Adv Ecol Res 30:1-67.

Alongi DM (2008) Mangrove forests: Resilience, protection from tsunamis, and responses to global climate change. Estuarine Coastal Shelf Sci 76:1-13.

Alongi DM, Boto KG, Robertson AI (1992) Nitrogen and phosphorus cycles. In: Robertson AI, Alongi DM (eds) Tropical Mangrove Ecosystems. American Geophysical Union, Washington, DC.

Ball MC (2009) Photosynthesis in mangroves. Wetlands Australia 6:12-22.

Ball MC (1988) Ecophysiology of mangroves. Trees-Struct Funct 2:129-142.

Ball MC (1996) Comparative ecophysiology of mangrove forest and tropical lowland moist rainforest. In: Mulkey SS, Chazdon RL, Smith AP (eds) Tropical forest plant ecophysiology Springer, Boston, Massachusetts, pp 461-496.

Ball MC, Farquhar GD (1984) Photosynthetic and stomatal responses of two mangrove species, *Aegiceras corniculatum* and *Avicennia marina*, to long term salinity and humidity conditions. Plant Physiol 74:1-6.

Barr JG, DeLonge MS, Fuentes JD (2014) Seasonal evapotranspiration patterns in mangrove forests. J Geophys Res Atmos 119:3886-3899.

Barr JG, Fuentes JD, Engel V, Zieman JC (2009) Physiological responses of red mangroves to the climate in the Florida Everglades. J Geophys Res Biogeosci 114:G02008.

Bates D, Mächler M, Bolker B, Walker S. (2015) Fitting linear fixed-effects models using lme4. J Stat Softw 67:1-48.

Bjorkman O, Demmig B, Andrews TJ (1988) Mangrove photosynthesis: response to high-irradiance stress. Funct Plant Bio 15:43-61.

Bouillon S, Borges AV, Castañeda-Moya E, Diele K, Dittmar T, Duke NC, Kristensen E, Lee SY, Marchand C, Middleburg JJ, Rivera-Monroy VH, Smith TJ, III., Twilley RR (2008) Mangrove production and carbon sinks: A revision of global budget estimates. Global Biogeochem Cycles. 22:GB2013.

Cardona-Olarte P, Krauss KW, Twilley RR (2013) Leaf gas exchange and nutrient use efficiency help explain the distribution of two Neotropical mangroves under contrasting flooding and salinity. Int J For Res 2013:1-10. doi:10.1155/2013/524625

Cardona-Olarte P, Twilley RR, Krauss KW, Rivera-Monroy VH (2006) Responses of neotropical mangrove seedlings grown in monoculture and mixed culture under treatments of hydroperiod and salinity. Hydrobiologia 569:325-341.

Castañeda-Moya E, Rivera-Monroy VH, Chambers RM, Zhao X, Lamb-Wotton L, Gorsky E, Gaiser EE, Troxler TG, Kominoski J, Hiatt M (2020) Hurricanes fertilize mangrove forests in the Gulf of Mexico (Florida Everglades, USA). PNAS 117:4831-4841.

Castañeda-Moya E, Twilley RR, Rivera-Monroy VH, Marx BD, Coronado-Molina C, Ewe SML (2011) Patterns of root dynamics in mangrove forests along environmental gradients in the Florida Coastal Everglades, USA. Ecosystems 14:1178-1195.

Castañeda-Moya E, Twilley RR, Rivera-Monroy VH (2013) Allocation of biomass and net primary productivity of mangrove forests along environmental gradients in the Florida Coastal Everglades, USA. For Ecol Manage 307:226-241.

954 Castañeda-Moya E, Rivera-Monroy VH, Twilley RR (2006) Mangrove zonation in the dry life
955 zone of the Gulf of Fonseca, Honduras. Estuaries Coasts 29, 751–764.
956 Chambers LG, Davis SE, Troxler T, Boyer JN, Downey-Wall A, Scinto LJ (2014)
957 Biogeochemical effects of simulated sea level rise on carbon loss in an Everglades
958 mangrove peat soil. Hydrobiologia 726:195-211.
959 Chapin FS, Bloom AJ, Field CB, Waring RH (1987) Plant responses to multiple environmental
960 factors. BioScience 37:49-57.
961 Chapin FS, Moilanen L (1991) Nutritional controls ver nitrogen and phosphorus resorption from
962 Alaskan birch leaves. Ecology 72:709-715.
963 Cheeseman J, Herendeen L, Cheeseman A, Clough B (1997) Photosynthesis and
964 photoprotection in mangroves under field conditions. Plant Cell Environ 20:579-588.
965 Cheeseman J, Lovelock C (2004) Photosynthetic characteristics of dwarf and fringe *Rhizophora*
966 *mangle* L. in a Belizean mangrove. Plant Cell Environ 27:769-780.
967 Childers DL (2006) A synthesis of long-term research by the Florida Coastal Everglades LTER
968 Program. Hydrobiologia. 569:531-544.
969 Childers DL, Boyer JN, Davis SE, Madden CJ, Rudnick DT, Sklar FH (2006) Relating
970 precipitation and water management to nutrient concentrations in the oligotrophic
971 “upside-down” estuaries of the Florida Everglades. Limnol Oceanogr 51:602-616.
972 Cintron G, Lugo AE, Douglas D, Pool J, Morris G (1978) Mangroves of Arid Environments in
973 Puerto Rico and Adjacent Islands. Biotropica 10:110-121.
974 Clough B, Sim R (1989) Changes in gas exchange characteristics and water use efficiency of
975 mangroves in response to salinity and vapour pressure deficit. Oecologia 79:38-44.
976 Cornelissen JH, Lavorel S, Garnier E, Díaz S, Buchmann N, Gurvich DE, Reich PB, Ter Steege
977 H, Morgan HD, Van Der Heijden MG, Pausas JG (2003) A handbook of protocols for
978 standardised and easy measurement of plant functional traits worldwide. Aust J Bot
979 51:335-80.
980 Craine JM, Brooksheir ENJ, Cramer MD, Hasselquist NJ, Koba K, Marin-Spiotta E, Wang L
981 (2015) Ecological interpreations of nitrogen isotope ratios of terrestrial plans and soils
982 Plant Soil 396:1-26.
983 Donato DC, Kauffman JB, Murdiyarso D, Kurnianto S, Stidham M, Kanninen M (2011)
984 Mangroves among the most carbon-rich forests in the tropics. Nat Geosci 4:293-297.
985 Duever MJ, Meeder JF, Meeder LC, McCollom JM (1994) The climate of South Florida and its
986 role in shaping the Everglades ecosystem. In: Davis SM,Ogden JC (eds) Everglades:
987 The Ecosystem and Its Restoration. St. Lucie Press, Delray Beach, Florida, pp 225-248.
988 Dlugokencky E, Tans P (2020) Trends in Atmospheric Carbon Dioxide. NOAA/GML
989 www.esrl.noaa.gov/gmd/ccgg/trends/
990 Ellison AM, Farnsworth EJ (1997) Simulated sea level change alters anatomy, physiology,
991 growth, and reproduction of red mangrove (*Rhizophora mangle* L.). Oecologia 112:435-
992 446.
993 Ewe SM, Gaiser EE, Childers DL, Iwaniec D, Rivera-Monroy VH, Twilley RR (2006) Spatial and
994 temporal patterns of aboveground net primary productivity (ANPP) along two freshwater-
995 estuarine transects in the Florida Coastal Everglades. Hydrobiologia 569:459-474.
996 Farnsworth EJ, Ellison AM (1996) Sun-shade adaptability of the red mangrove, *Rhizophora*
997 *mangle* (Rhizophoraceae): Changes through ontogeny at several levels of biological
998 organization. Amer J Bot 83:1131-1143.
999 Feller IC (1995) Effects of nutrient enrichment on growth and herbivory of dwarf red mangrove
1000 (*Rhizophora mangle*). Ecol Monogr 65:477-505.
1001 Feller IC, McKee KL, Whigham DF, O'Neill JP (2003a) Nitrogen vs. phosphorus limitation across
1002 an ecotonal gradient in a mangrove forest. Biogeochemistry 62:145-175.

1003 Feller IC, Whigham DF, McKee KL, Lovelock CE (2003b) Nitrogen limitation of growth and
1004 nutrient dynamics in a disturbed mangrove forest, Indian River Lagoon, Florida.
1005 Oecologia 134:405-414.
1006 Field CD (1984) Ions in mangroves. In: Teas HJ (ed) Physiology and management of
1007 mangroves. Springer, Dordrecht, Netherlands, pp 43-48.
1008 Field CD (1995) Impact of expected climate change on mangroves. Hydrobiologia 295:75-81.
1009 Fogel M, Wooller M, Cheeseman J, Smallwood B, Roberts Q, Romero I, Jacobsen Meyers M
1010 (2008) Unusually negative nitrogen isotopic compositions ($\delta^{15}N$) of mangroves and
1011 lichens in an oligotrophic, microbially-influenced ecosystem. Biogeosci Discuss 5:1693-
1012 1704.
1013 Fry B, Bern A, Ross M, Meeder J (2000) $\delta^{15}N$ studies of nitrogen use by the red mangrove,
1014 Rhizophora mangle L. in south Florida. Estuarine Coastal Shelf Sci 50:291-296.
1015 Garten CTJ (1993) Variation in foliar ^{15}N abundance and the availability of soil nitrogen on
1016 Walker Branch watershed. Ecology 74:2098-2113.
1017 Giri C, Ochieng E, Tieszen LL, Zhu Z, Singh A, Loveland T, Masek J, Duke NC (2011) Status
1018 and distribution of mangrove forests of the world using earth observation satellite data.
1019 Global Ecol Biogeogr 20:154-159.
1020 Gleeson SK, Tilman D (1992) Plant allocation and the multiple limitation hypothesis. Am Nat
1021 139:1322-1343.
1022 Golley F, Odum HT, Wilson RF (1962) The structure and metabolism of a Puerto Rican red
1023 mangrove forest in May. Ecology 43:9-19.
1024 Güsewell S (2004) N: P ratios in terrestrial plants: variation and functional significance. New
1025 phytol 164:243-266.
1026 He B, Lai T, Fan H, Wang W, Zheng H (2007) Comparison of flooding-tolerance in four
1027 mangrove species in a diurnal tidal zone in the Beibu Gulf. Estuarine Coastal Shelf Sci
1028 74:254-262.
1029 He D, Rivera-Monroy VH, Jaffé R, Zhao X (2020) Mangrove leaf species-specific isotopic
1030 signatures along a salinity and phosphorus soil fertility gradients in a subtropical estuary.
1031 Estuarine Coastal Shelf Sci 106768.
1032 Högberg P (1997) ^{15}N natural abundance in soil-plant systems. New Phytol 137:179-203.
1033 Hoppe-Speer SC, Adams JB, Rajkaran A, Bailey D (2011) The response of the red mangrove
1034 *Rhizophora mucronata* Lam. to salinity and inundation in South Africa. Aquat Bot 95:71-
1035 76.
1036 Hughes CE, Binning P, Willgoose GR (1998) Characterisation of the hydrology of an estuarine
1037 wetland. J Hydrol 211:34-49.
1038 Jennerjahn TC, Ittekkot V (2002) Relevance of mangroves for the production and deposition of
1039 organic matter along tropical continental margins. Naturwissenschaften. 89:23-30.
1040 Kattge J, Bönisch G, Díaz S, Lavorel S, Prentice IC, Leadley P, Tautenhahn S, Werner GD,
1041 Aakala T, Abedi M (2020) TRY plant trait database–enhanced coverage and open
1042 access. Glob Change Biol. 26:119-188.
1043 Koch MS, Snedaker SC (1997) Factors influencing *Rhizophora mangle* L. seedling development
1044 in Everglades carbonate soils. Aquat Bot 59:87-98.
1045 Kozlowski TT (1997) Responses of woody plants to flooding and salinity. Tree Physiol 17:490-
1046 490.
1047 Krauss KW, McKee KL, Lovelock CE, Cahoon DR, Saintilan N, Reef R, Chen L (2014) How
1048 mangrove forests adjust to rising sea level. New Phytol 202:19-34.
1049 Krauss KW, Twilley RR, Doyle TW, Gardiner ES (2006) Leaf gas exchange characteristics of
1050 three neotropical mangrove species in response to varying hydroperiod. Tree Physiol
1051 26:959-968.
1052 Kuznetsova A, Brockhoff PB, Christensen RHB (2017) lmerTest Package: Tests in Linear Mixed
1053 Effects Models. J Stat Softw 82:13.

Lambers H, Chapin FS, Pons TL (eds) (2008) Plant physiological ecology. Springer, New York, New York.

Lamers LPM, Govers LL, Janssen ICJM, Geurts JJM, Van der Welle MEW, Van Katwijk MM, Van del Heide T, Roelofs JGM, Smolders AJP (2013) Sulfide as a soil phytotoxin - a review. Front Plant Sci 4:1-14.

Lin G, Sternberg LSL (1992) Comparative study of water uptake and photosynthetic gas exchange between scrub and fringe red mangroves, *Rhizophora mangle* L. Oecologia 90:399-403.

Lopes D, Tognella M, Falqueto A, Soares M (2019) Salinity variation effects on photosynthetic responses of the mangrove species *Rhizophora mangle* L. growing in natural habitats. Photosynthetica 57:1142-1155.

Loveless CM (1959) A study of the vegetation in the Florida Everglades. Ecology 40:2-9.

Lovelock CE (2008) Soil respiration and belowground carbon allocation in mangrove forests. Ecosystems 11:342-354.

Lovelock CE, Feller I (2003) Photosynthetic performance and resource utilization of two mangrove species coexisting in hypersaline scrub forest. Oecologia 134:455-462.

Lovelock CE, Atwood T, Baldock J, Duarte CM, Hickey S, Lavery P, Masque P, Macreadie PI, Ricart AM, Serrano O, Steven A (2017) Assesing the risk of carbon dioxide emissions from blue carbon ecosystems. Front Ecol Environ 15:257-265.

Lüdecke D (2018) sjPlot: Data visualization for statistics in social science. R package version 2. https://cran.r-project.org/web/packages/sjPlot/

Lugo AE, Medina E, Cuevas E, Cintrón G, Nieves ENL, Novelli YS (2007) Ecophysiology of a mangrove forest in Jobos Bay, Puerto Rico. Carib J Sci 43:200-219.

Lugo AE, Snedaker SC (1974) The ecology of mangroves. Ann Rev Ecol System 5:39-64.

Marshall JD, Brooks JR, Lajtha K (2007) Stable isotopes in ecology and environmental science. In: Michener R, Lajtha K (eds) Sources of variation in the stable isotopic composition of plants .Blackwell, Singapore, pp 22-60.

McKee KL (1993) Soil physicochemical patterns and mangrove species distribution-reciprocal effects? J Ecol 81:477-487.

McKee KL (2011) Biophysical controls on accretion and elevation change in Caribbean mangrove ecosystems. Estuarine Coastal Shelf Sci 91:475-483.

McKee KL, Cahoon DR, Feller IC (2007) Caribbean mangroves adjust to rising sea level through biotic controls on change in soil elevation. Global Ecol Biogeogr 16:545-556.

McKee KL, Feller IC, Popp M, Wanek W (2002) Mangrove isotopic ($\delta^{15}N$ and $\delta^{13}C$) fractionation across a nitrogen vs. phosphorus limitation gradient. Ecology 83:1065-1075.

Mcleod E, Chmura GL, Bouillon S, Salm R, Bjork M, Duarte CM, Lovelock CE, Schlesinger WH, Silliman BR (2011) A blueprint for blue carbon: Toward an improved understanding of the role of vegetated coastal habitats in sequestering CO_2. Front Ecol Environ 9:552-560.

Medina E (1999) Mangrove physiology: the challenge of salt, heat, and light stress under recurrent flooding. In: Yañez-Arancibia A, Lara-Domínguez L (eds) Ecosistemas de manglar en América tropical. Instituto de Ecología A.C. México, UICN/ORMA, Costa Rica, NOAA/NMFS Silver Spring, MD USA. pp 109-126.

Medina E, Cuevas E, Lugo AE (2010) Nutrient relations of dwarf *Rhizophora mangle* L. mangroves on peat in eastern Puerto Rico. Plant ecolog 207:13-24.

Medina E, Francisco M (1997) Osmolality and $\delta^{13}C$ of leaf tissues of mangrove species from environments of contrasting rainfall and salinity. Estuarine Coastal Shelf Sci 45:337-344.

Medina E, Francisco M, Quilice A (2008) Isotopic signatures and nutrient relations of plants inhabiting brackish wetlands in the northeastern coastal plain of Venezuela. Wetlands Ecol Manage 16:51.

1103 Mendelssohn I, McKee K (2000) Saltmarshes and mangroves. In: Barbour MG, Billings WD
1104 (eds) North American terrestrial vegetation. Cambridge University Press, New York, NY,
1105 pp 501-536.
1106 Michot B, Meselhe EA, Rivera-Monroy VH, Coronado-Molina C, Twilley RR (2011) A tidal creek
1107 water budget: estimation of groundwater discharge and overland flow using hydrologic
1108 modeling in the southern Everglades. Estuarine Coastal Shelf Sci 93:438-448.
1109 Murdiyarso D, Purbopuspito J, Kauffman JB, Warren MW, Sasmito SD, Donato DC, Manuri S,
1110 Krisnawati H, Taberima S, Kurnianto S (2015) The potential of Indonesian mangrove
1111 forests for global climate change mitigation. Nat Clim Change 5:1089-1092.
1112 Naidoo G (1983) Effects of flooding on leaf water potential ans stomatal resistance in *Bruguiera*
1113 gymnorrhiza (L.) LAM. New Phytol 93:369-373.
1114 Neubauer SC, Franklin RB, Berrier DJ (2013) Saltwater intrusion into tidal freshwater marshes
1115 alters the biogeochemical processing of organic carbon. Biogeosciences Discuss
1116 10:10685-10720.
1117 Nickerson NH, Thibodeau FR (1985) Association between porewater sulfide concentrations and
1118 distribution of mangroves. Biogeochemistry 1:183-192.
1119 O'Leary MH (1988) Carbon isotopes in photosynthesis. BioScience. 38:328-336.
1120 Parida AK, Jha B (2010) Salt tolerance mechanisms in mangroves: a review. Trees-Struct Funct
1121 24:199-217.
1122 Pezeshki S, DeLaune R, Patrick Jr W (1990a) Flooding and saltwater intrusion: Potential effects
1123 on survival and productivity of wetland forests along the U.S. Gulf Coast. For Ecol
1124 Manage 33:287-301.
1125 Pezeshki S, DeLaune R, Patrick Jr W (1990b) Differential response of selected mangroves to
1126 soil flooding and salinity: gas exchange and biomass partitioning. Can J For Res 20:869-
1127 874.
1128 Pezeshki SR, DeLaune RD (2012) Soil oxidation-reduction in wetlands and its impact on plant
1129 functioning. Biology 1:196-221.
1130 Potts M (1979) Nitrogen fixation (acetylene reduction) associated with communities of
1131 heterocystous and non-heterocystous blue-green algae in mangrove forests of Sinai.
1132 Oecologia 39:359-373.
1133 Pugnaire FI, Chapin F.S. (1993) Controls over nutrient resorption from leaves of evergreen
1134 Mediterranean species. Ecology 4:124-129.
1135 R Core Team (2018) R: a language and environment for statiscal computing. R foundation for
1136 staistical computing. Vienna, Austria. www.r-project.org
1137 Reef R, Lovelock CE (2015) Regulation of water balance in mangroves. Ann Bot 115:385-395.
1138 Reis CRG, Nardoto GB, Oliveira RS (2017a) Global overview on nitrogen dynamics in
1139 mangroves and consequences of increasing nitrogen availability for these systems.
1140 Plant Soil 410:1-19.
1141 Reis CRG, Nardoto GB, Rochelle ALC, Vieira SA, Oliveira RS (2017b) Nitrogen dynamics in
1142 subtropical fringe and basin mangrove forests inferred from stable isotopes. Oecologia
1143 183:841-848.
1144 Ribeiro, RDA, Rovai AS, Twilley RR, Castañeda-Moya E (2019). Spatial variability of mangrove
1145 primary productivity in the neotropics Ecosphere 10:e02841.
1146 Rivera-Monroy VH, Danielson TM, Castañeda-Moya E, Marx BD, Travieso R, Zhao X, Gaiser
1147 EE, Farfan LM (2019) Long-term demography and stem productivity of Everglades
1148 mangrove forests (Florida, USA): Resistance to hurricane disturbance. For Ecol Manage
1149 440:79-91.
1150 Robinson D (2001) $\delta^{15}N$ as an integrator of the nitrogen cycle. Trends Ecol Evol 16:153-162.
1151 Rodrigues DP, Hamacher C, Estrada GCD, Soares MLG (2015) Variability of carbon content in
1152 mangrove species: Effect of species, compartments and tidal frequency. Aquat Bot
1153 120:346-351

R Core Team (2018) R: a language and environment for statiscal computing. R foundation for staistical computing. Vienna, Austria. www.r-project.org

Ross MS, Meeder JF, Sah JP, Ruiz PL, Telesnicki GJ (2000) The southeast saline Everglades revisited: 50 years of coastal vegetation change. J Veg Sci 11:101-112.

Rovai AS, Twilley RR, Castañeda-Moya E, Riul P, Cifuentes-Lara M, Manrow-Villalobos M, Horta PA, Simonassi JC, Fonseca AL, Pagliosa PR (2018) Global controls of carbon storage in mangrove soils. Nat Clim Change 8:534-538.

Rovai AS, Twilley RR, Castañeda-Moya E, Rivera-Monroy V, Williams A, Simard M, Cifuentes-Lara M, Lewis RR, Crooks S, Horta PA, Schaeffer-Novelli Y, Cintron G, Pozo-Cajas M, Pagliosa PR (2016) Scaling mangrove aboveground biomass from site-level to continental-scale. Global Ecol Biogeogr 25:286-298.

Schneider CA, Rasband WS, Eliceiri KW (2012) NIH Image to ImageJ: 25 years of image analysis. Nat Methods 9:671-675.

Scholander P (1968) How mangroves desalinate seawater. Physiol Plant 21:251-261.

Scholander P, Hammel H, Hemmingsen E, Garey W (1962) Salt balance in mangroves. Plant Physiol 37:722.

Simard M, Fatoyinbo L, Smetanka C, Rivera-Monroy VH, Castañeda-Moya E, Thomas N, Van der Stocken T (2019) Mangrove canopy height globally related to precipiation temperature and cyclone frequency. Nat Geosci 12:40-45.

Simard M, Zhang K, Rivera-Monroy V, Ross MS, Ruiz PL, Castañeda-Moya E, Twilley RR, Rodriguez E (2006) Mapping height and biomass of mangrove forests in Everglades National Park with SRTM elevation data. Photogramm Eng Remote Sens 72:299-311.

Soares MG, Tognella MP, Cuevas E, Medina E (2015) Photosynthetic capacity and intrinsic water-use efficiency of *Rhizophora mangle* at its southernmost western Atlantic range. Photosynthetica 53:464-470.

Sobrado M (2000) Relation of water transport to leaf gas exchange properties in three mangrove species. Tree-Struct Funct 14:258-262.

Sutula M, Day JW, Cable JE, Rudnick D (2001) Hydrological and nutrient budgets of freshwater and estuarine wetlands of Taylor Slough in southern Everglades, Florida (U.S.A.). Biogeochemistry 56:287-310.

Tully K, Gedan K, Epanchin-Niell R, Strong A, Bernhardt ES, BenDor T, Mitchell M, Kominoski J, Jordan TE, Neubauer SC, Weston NB (2019) The invisible flood: The chemistry, ecology, and social implications of coastal saltwater intrusion. BioScience 69:368-378.

Thom BG (1982) Mangrove ecology - a geomorphological perspective. In: Clough BF (ed) Mangrove Ecosystems in Australia. Australian National University Press, Canberra, pp 3-17.

Tomlinson PB (2016) The botany of mangroves. Cambridge University Press, Cambridge, Massachusetts.

Troxler TG (2007) Patterns of phosphorus, nitrogen and $\delta^{15}N$ along a peat development gradient in a coastal mire, Panama. J Trop Ecology 23:683-691.

Twilley RR (1995) Properties of mangrove ecosystems related to the energy signature of coastal environments. In: Hall CAS (ed) Maximum power: the ideas and applications of H. T. Odum. University Press of Colorado, Niwot, Colorado, pp 43-62.

Twilley RR, Castañeda-Moya E, Rivera-Monroy VH, Rovai A (2017) Productivity and carbon dynamics in mangrove wetlands. In: Rivera-Monroy VH, Lee SY, Kristensen E, Twilley RR (eds) Mangrove ecosystems: A global biogeographic perspective. Springer International, pp 113-162.

Twilley RR, Chen RH, Hargis T (1992) Carbon sinks in mangroves and theirs implications to carbon budget of tropical coastal ecosystems. Water Air Soil Pollut 64:265-288.

Twilley RR, Lugo AE, Patterson-Zucca C (1986) Litter production and turnover in basin mangrove forests in southwest Florida. Ecology 67:670-683.

1205 Twilley RR, Rivera-Monroy V, Rovai AS, Castañeda-Moya E, Davis SE, III. (2019) Mangrove
1206 biogeochemistry at local to global scales using ecogeomorphic approaches. In: Perillo
1207 GME, Wolanski E, Cahoon DR, Hopkinson CS (eds) Coastal Wetlands: An Integrated
1208 Ecosystem Approach.Elsevier, pp 717-785.
1209 Twilley RR, Rivera-Monroy VH, Chen R, Botero L (1998) Adapting and ecological mangrove
1210 model to simulate trajectories in restoration ecology. Mar. Poll. Bull. 37:404-419.
1211 Uncles R, Gong W-K, Ong J-E (1992) Intratidal fluctuations in stratification within a mangrove
1212 estuary. In: Martens E, Jaccarini V (eds) The Ecology of Mangrove and Related
1213 Ecosystems. Springer, pp 163-171.
1214 Vitousek P (1982) Nutrient cycling and nutrient use efficiency. Am Nat 119:553-572.
1215 Wanless H (1998) Mangroves, hurricanes, and sea level rise. South Florida Study Group, The
1216 Conservancy, Naples, Florida
1217 Wassen MJ, Olde Venterink HG, de Swart EO (1995) Nutrient concentrations in mire vegetation
1218 as a measure of nutrient limitation in mire ecosystems. J Veg Sci 6:5-16.
1219 Werner A, Stelzer R (1990) Physiological responses of the mangrove *Rhizophora mangle* grown
1220 in the absence and presence of NaCl. Plant Cell Environ 13:243-255.
1221 Wolanski E (1992) Hydrodynamics of mangrove swamps and their coastal waters.
1222 Hydrobiologia 247:141-161.
1223 Woodroffe C (1992) Mangrove sediments and geomorphology. In: Robertson AI and Alongi DM
1224 (eds) Tropical Mangrove Ecosystems. American Geophysical Union, Washington, DC,
1225 pp 7-41.
1226 Wooller M, Smallwood B, Scharler U, Jacobson M, Fogel M (2003) A taphonomic study of δ13C
1227 and δ15N values in Rhizophora mangle leaves for a multi-proxy approach to mangrove
1228 palaeoecology. Org Geochem 34:1259-1275.
1229 Yu M, Rivera-Ocasio E, Heartsill-Scalley T, Davila-Casanova D, Rios-López N, Gao Q. (2019)
1230 Landscape-level consequences of rising sea-level on coastal wetlands: saltwater
1231 intrusion drives displacement and mortality in the twenty-first century. Wetlands 39:1343-
1232 1355.
1233 Zhao X, Rivera-Monroy V, Wang H, Xue ZG, Tsai CF, Wilson C, Castañeda-Moya E (2020)
1234 Modeling soil porewater salinity in mangrove forests (Everglades, Florida, USA)
1235 impacted by hydrological restoration and a warming climate. Ecol Model 436:109272

1236

TABLES

Table 1: Mean (± 1 SE) soil surface elevation, bedrock elevation, and soil depth, for open water, mangrove island edge and center habitats for the fringe and interior scrub mangrove areas at TS/Ph-7 in southeastern Florida Coastal Everglades. Elevation measurements are referenced to the North American Vertical Datum 1988 (NAVD88). Letters denote statistically different groupings via Tukey HSD post-hoc test ($p < .05$).

Mangrove Location	Habitat	Soil Surface Elevation (NAVD88, m)	Bedrock Elevation (NAVD88, m)	Soil depth (m)
Fringe	Open water	-0.63 ± 0.05^{C}	-1.84 ± 0.05^{A}	1.22 ± 0.05^{C}
	Island edge	-0.41 ± 0.03^{B}	-1.83 ± 0.02^{A}	1.43 ± 0.05^{BC}
	Island center	-0.14 ± 0.02^{A}	-1.86 ± 0.06^{A}	1.72 ± 0.05^{A}
Interior	Open water	-0.84 ± 0.02^{D}	-2.01 ± 0.15^{A}	1.18 ± 0.14^{C}
	Island edge	-0.49 ± 0.03^{B}	-1.78 ± 0.04^{A}	1.39 ± 0.04^{C}
	Island center	-0.15 ± 0.02^{A}	-1.77 ± 0.03^{A}	1.62 ± 0.03^{AB}

1244 **Table 2:** Seasonal variation in water levels, surface water and porewater salinity measured in
1245 mangrove island habitats at scrub *R. mangle* dominated mangroves at TS/Ph-7 in southeastern
1246 Florida Everglades. Means (± 1 SE) with different letters within each column denoting
1247 significant differences among groups (Tukey HSD post hoc, $p < .05$).

1248

Season	Habitat	Water level (cm)	Surface water salinity (ppt)	Porewater salinity (ppt)
Dry	Edge	33.5 ± 1.9^{A}	16.11 ± 1.16^{A}	24.22 ± 0.44^{A}
	Center	10.1 ± 1.9^{B}	21.14 ± 1.51^{B}	20.83 ± 0.44^{B}
Wet	Edge	40.2 ± 1.9^{C}	15.31 ± 1.16^{A}	26.00 ± 0.44^{C}
	Center	15.5 ± 1.9^{B}	14.41 ± 1.47^{A}	22.22 ± 0.44^{D}

Table 3. Leaf functional traits, carbon and nutrient contents and N:P ratios, nitrogen and phosphorus resorption efficiencies and bulk isotopic signatures, and intrinsic intracellular CO_2 concentrations (c_i) and intrinsic water use-efficiency (*WUE*) (calculated from ^{13}C fractionation) for scrub *R. mangle* leaves collected at mangrove island habitats at TS/Ph-7 during the dry and wet seasons of 2019. Means (± 1 SE) with different letters across each row denoting significantly different groups (Tukey HSD test, $p < .05$).

Leaf Trait	Dry season		Wet season	
	Edge	Center	Edge	Center
Leaf dry mass (g)	0.64 ± 0.02^{A}	0.65 ± 0.02^{A}	0.69 ± 0.02^{A}	0.70 ± 0.02^{A}
Leaf area (cm^2)	24.9 ± 0.7^{A}	25.5 ± 0.7^{A}	26.0 ± 1.4^{A}	27.3 ± 0.9^{A}
SLA ($g\ cm^{-2}$)	28.97 ± 0.66^{A}	39.79 ± 0.68^{A}	37.33 ± 0.40^{A}	40.04 ± 1.71^{A}
LWC (%)	65.7 ± 0.4^{A}	65.4 ± 0.5^{A}	63.6 ± 0.5^{A}	64.0 ± 0.8^{A}
Total C ($mg\ g^{-1}$)	450.9 ± 5.7^{A}	441.4 ± 1.0^{A}	428.7 ± 17.7^{A}	444.0 ± 1.0^{A}
Total N ($mg\ g^{-1}$)	9.8 ± 0.2^{AB}	10.2 ± 0.3^{A}	8.4 ± 0.5^{B}	9.0 ± 0.3^{AB}
Total P ($mg\ g^{-1}$)	0.50 ± 0.01^{AB}	0.55 ± 0.04^{A}	0.42 ± 0.01^{B}	0.46 ± 0.02^{AB}
Atomic N:P	41.7 ± 1.9	40.0 ± 0.1	43.5 ± 3.7	42.5 ± 2.1
N resorption (%)	60.0 ± 0.4	62.8 ± 0.5	60.8 ± 2.8	62.9 ± 1.5
P resorption n (%)	78.6 ± 0.2	74.3 ± 3.2	75.5 ± 0.4	73.2 ± 6.2
$\delta^{13}C$ (‰)	-25.5 ± 0.1^{AB}	-25.1 ± 0.1^{A}	-25.8 ± 0.1^{B}	-25.9 ± 0.2^{AB}
c_i ($\mu mol\ mol^{-1}$)	228.1 ± 2.2^{AB}	219.9 ± 1.8^{B}	233.3 ± 1.1^{A}	235.3 ± 3.6^{A}
WUE ($mmol\ mol^{-1}$)	0.1124 ± 0.0014^{AB}	0.1175 ± 0.0012^{B}	0.1092 ± 0.0007^{A}	0.1080 ± 0.0022^{A}
$\delta^{15}N$ (‰)	-5.3 ± 0.5^{B}	-0.4 ± 0.4^{A}	-4.2 ± 1.0^{AB}	-0.8 ± 1.5^{A}

1256 **FIGURES**

1257

1258 **Figure 1. A)** Photograph of TS/PH-7, showing scrub *R. mangle* tree islands which characterize
1259 the study site. Mangrove canopy heights are approximately 2 meters tall, facilitating canopy
1260 measurements of leaf physiology. Boardwalk (1.3 m height) is pictured for reference. **B)** Aerial
1261 view (Google Earth) of mangrove islands measured for this study within TS/Ph-7, near the
1262 mouth of the Taylor River in southeastern Florida Coastal Everglades, USA. The inset shows
1263 the location of TS/Ph-7 within the boundary of Everglades National Park. Colors indicate scrub
1264 mangroves and fringe and interior zones relative to the shoreline (i.e., Taylor River). Symbols
1265 denoted paired higher-elevation, center and lower-elevation, edge habitats for each mangrove
1266 island (squares and triangles, respectively).

1267

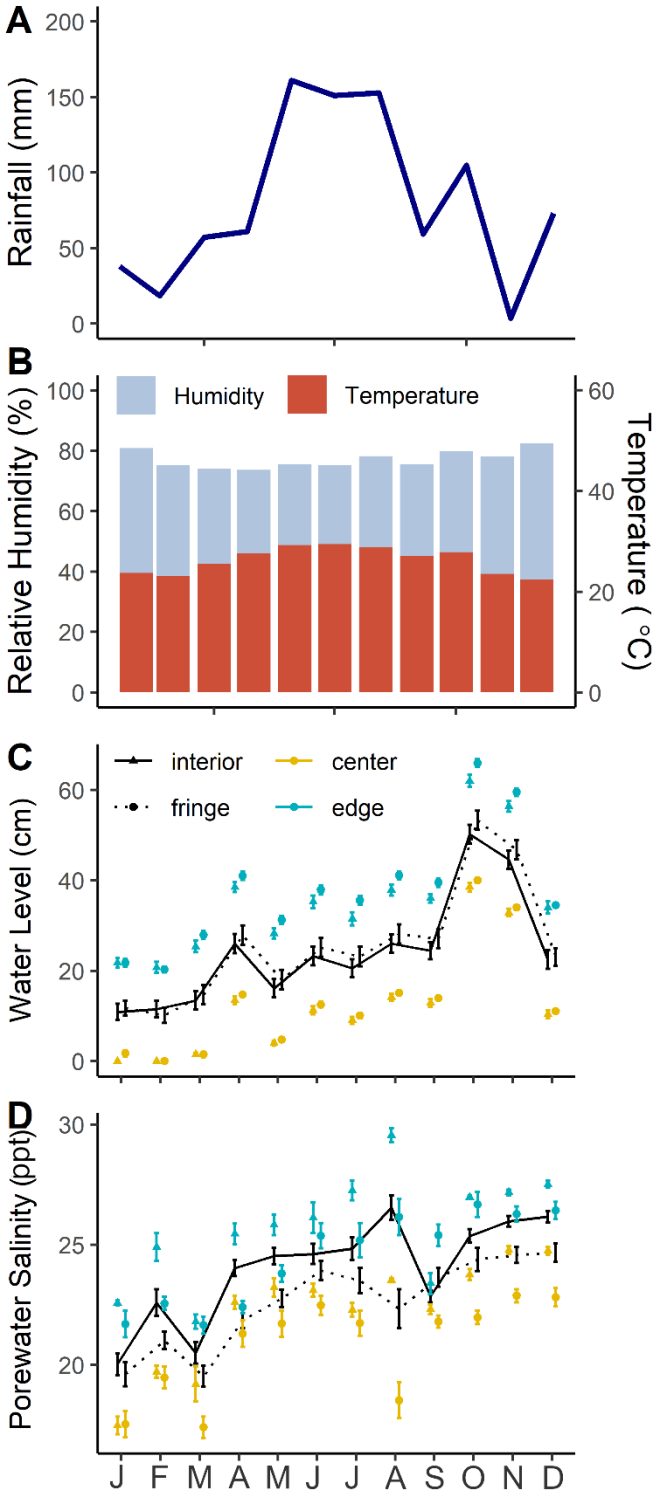

Figure 2. Environmental parameters for TS/Ph-7 for the 2019 calendar year. Cumulative monthly rainfall **(A)**, monthly average relative humidity and air temperature **(B)**, average (± 1 SE) water level **(C),** and average (± 1 SE) porewater salinity **(D)** measured at mangrove island habitats at the study site. Scrub mangroves from fringe and interior zones sampled during the study are shown in dotted and solid lines, respectively, whereas mangrove edge, and center

habitats are differentiated by color (teal and gold, respectively). Rainfall data **(A)** were obtained from a USGS-maintained rain gauge in Taylor River, which is part of the Everglades Depth Estimation Network (Skinner et al. 2009). Data for **B** were collected from an eddy covariance tower located at the study site. Water level **(C)** and porewater salinity **(D)** were measured for each island, at both the edge and center habitats, during monthly mangrove leaf photosynthesis measurements.

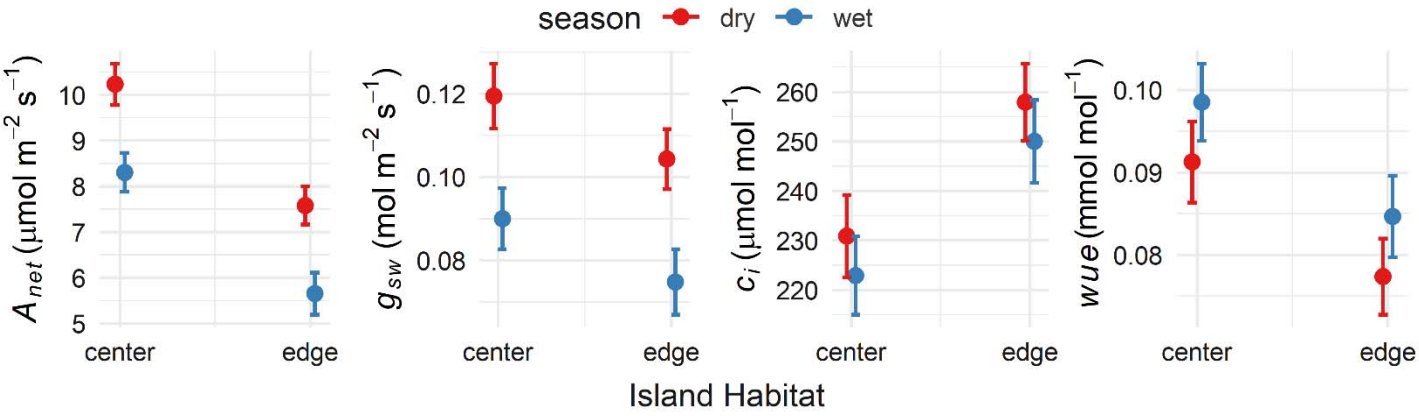

Figure 3. Predicted marginal mean (±95% confidence intervals) values of photosynthesis (A_{net}), stomatal conductance (g_{sw}), the concentration of intracellular CO_2 (c_i), and instantaneous water use efficiency (*wue*) by mangrove island habitat and season. The dry season is November to April, and the wet season is May to October. See supplemental material for complete model summaries.

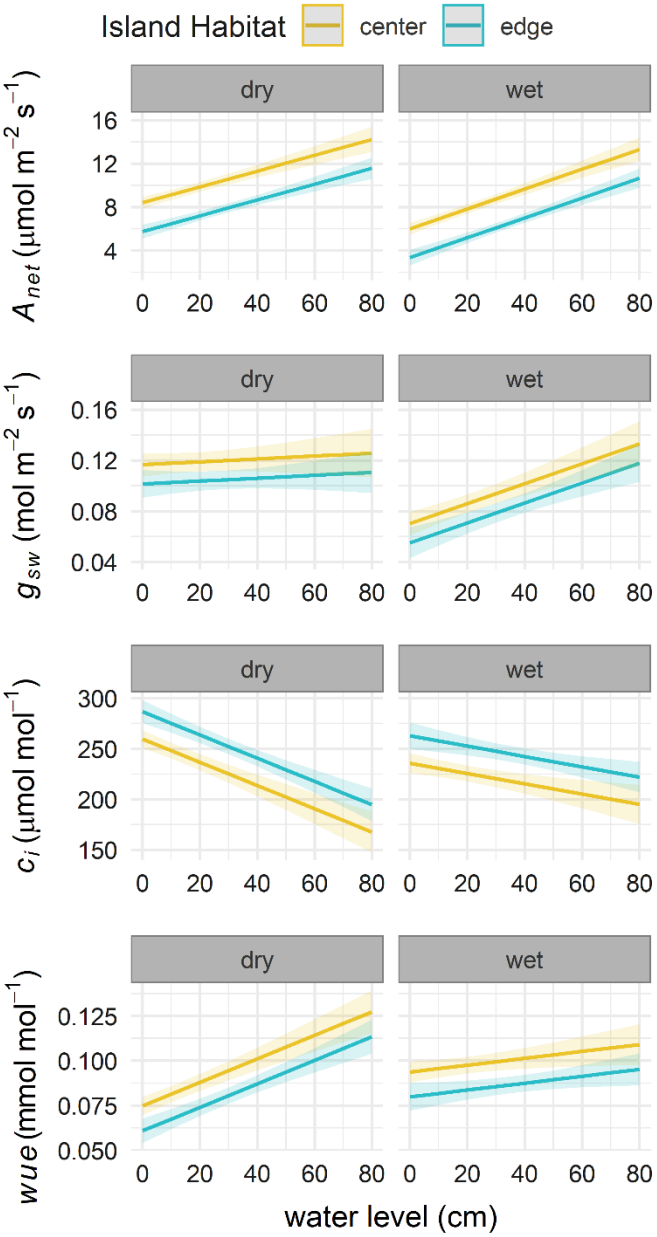

Figure 4. The effect of water level on leaf photosynthesis (A_{net}) and stomatal conductance (g_{sw}), the concentration of intracellular CO_2 (c_i), and instantaneous water use efficiency (*wue*) by season. Lines are habitat-specific predicted mean marginal mean values (± 95% confidence intervals) from linear mixed-effects models.

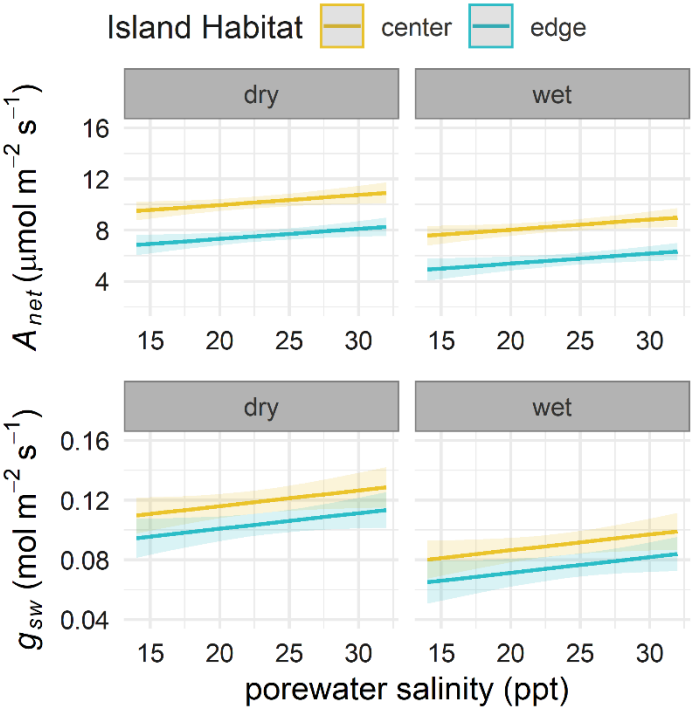

Figure 5. The effect of soil porewater salinity on leaf photosynthesis (A_{net}) and stomatal conductance (g_{sw}) by season. Porewater salinity was not included in the best-fitting models for c_i or *wue*. Lines are predicted mean marginal effects from linear mixed-effects models ± 95% confidence intervals (colored by island habitat).

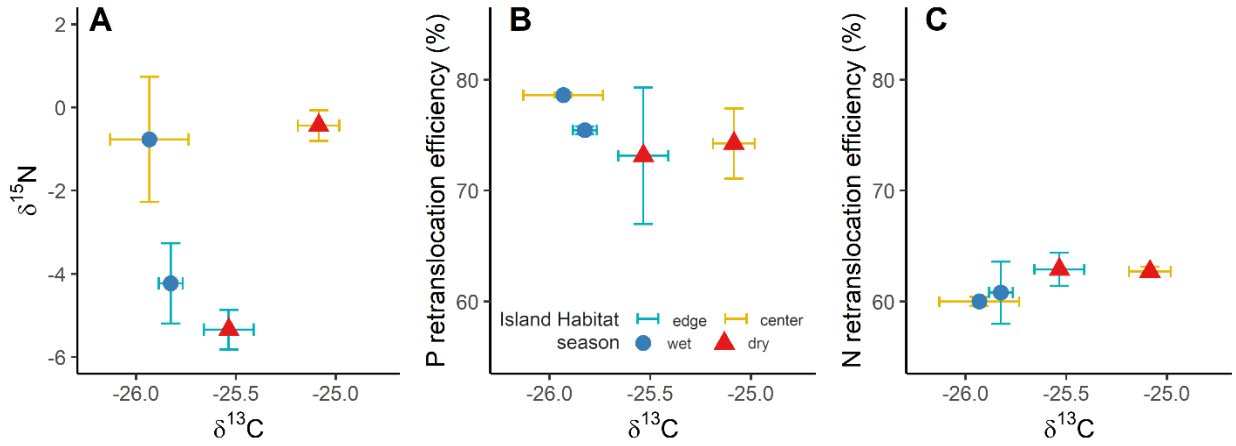

Figure 6. Mean (± 1 SE) leaf isotopic signatures and nutrient resorption efficiency by island habitat and season combination. A) the relationship between $\delta^{15}N$ and $\delta^{13}C$ in *R. mangle* green leaves, B) the relationship between N translocation efficiency and $\delta^{13}C$ for *R. mangle* green leaves, and C) the relationship between P resorption efficiency and $\delta^{13}C$ for *R. mangle* green leaves. Error bar colors denote island habitats, while point symbols show seasons.